

DTIC FILE COPY

DARPA ORDER 9526

2

AD-A217 840

ENHANCED CERIA SOLID ELECTROLYTE FUEL CELL DEVELOPMENT

**Reduction of Electronic Conductivity Permits use of a Solid Ceria Electrolyte
in High Efficiency High Power Density Fuel Cells at Temperatures Compatible
with Metallic Cell Hardware**

Prepared by

D. L. Maricle

International Fuel Cells
P.O. Box 739
195 Governors Highway
South Windsor, CT 06074

DTIC
ELECTE
FEB 08 1990
S D D

January 1990

FCR-10824

Final Technical Report

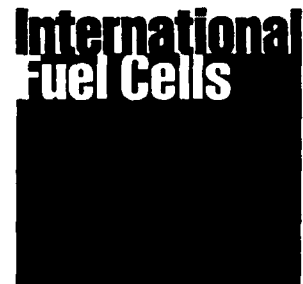
Contract Number N00014-88-C-0390

Prepared for

Defense Advanced Research Project Agency
1400 Wilson Blvd.
Arlington, VA 22209-2308

Office of Naval Research
800 North Quincy Street
Arlington, VA 2221

DISTRIBUTION STATEMENT A
Approved for public release
Distribution Unlimited



P.O. Box 739
195 Governors Highway
South Windsor, Connecticut 06074

90 02 06 006

ENHANCED CERIA SOLID ELECTROLYTE FUEL CELL DEVELOPMENT

**Reduction of Electronic Conductivity Permits use of a Solid Ceria Electrolyte
in High Efficiency High Power Density Fuel Cells at Temperatures Compatible with Me-
tallic Cell Hardware**

Prepared by

D. L. Maricle

**International Fuel Cells
P.O. Box 739
195 Governors Highway
South Windsor, CT 06074**

January 1990

FCR-10824

Final Technical Report

Contract Number N00014-88-C-0390

Prepared for

**Defense Advanced Research Project Agency
1400 Wilson Blvd.
Arlington, VA 22209-2308**

**Office of Naval Research
800 North Quincy Street
Arlington, VA 2221**

The views and conclusions contained in this document are those of the authors and should not be interpreted as necessarily representing the official policies, either expressed or implied, of the Defense Advanced Research Projects Agency or the U. S. Government.

Best Available Copy

TABLE OF CONTENTS

	Page
SUMMARY	1
INTRODUCTION	1
RESULTS	2
Task 1 Literature Search	2
Task 2 Experimental Evaluation of Dopants to Increase the Ratio of Ionic to Electronic Conductivity	2
2.1 Sample Preparation and Electrical Measurement Techniques	2
2.2 Verification of Improved Electrolytic Domain Boundary by AC Impedance Analysis	4
2.3 Optimization of Composition	6
2.4 Measurement of Activation Energy of Electronic and Ionic Conductivity	9
2.5 Analysis of Bulk and Grain Boundary Conductivities as a Function of Temperature	14
2.6 Impact of Grain Size on Electronic and Ionic Conductivity	17
2.7 New Compositions	16
Task 3 Experimental Evaluation of Barrier Layers to Increase the Ratio of Ionic to Electronic Conductivity	19
3.1 Evaluation of Zirconia as Grain Boundary Barrier Layer	19
Phase I Program Review	21
A. Recommended Approach	21
B. Calculated Cell Performance Parameters	21
REFERENCES	26
BIBLIOGRAPHY	27
DISTRIBUTION LIST	33
APPENDICES	34

LIST OF ILLUSTRATIONS

Figure	Page
1. (A) Schematic diagram of a complex impedance plot showing arcs due to three processes. (B) The equivalent circuit that gives rise to the three arcs shown in (A).	3
2. Total Conductivity as a Function of Oxygen Partial Pressure 700°C	5
3. Electrolytic Domain Boundary Vs. Dopant A Level at 700°C	7
4. Electronic Conductivity at $PO_2 = 10^{-23}$ Vs. Dopant A Level	8
5. Ionic Conductivity - Temperature Behavior Oxide B3 at $PO_2 = 10^{-1}$	10
6. Electric Conductivity Vs. PO_2 at 3 Temperatures Oxide B3	11
7. Electronic Conductivity - Temperature Behavior Oxide B3 at $PO_2 = 10^{-18}$	12
8. Temperature Behavior of Electrolytic Domain Boundary	13
9. Conductivity Vs. Temperature, $PO_2 = 0.1 Ce_{0.8}Gd_{0.2}O_{2-y}$	15
10. Conductivity *T Vs. Temperature, $PO_2 = 0.1$ Oxide B1	16
11. Conductivity Vs. Temperature, $PO_2 = 0.1$ Oxide B5	18
12. Conductivity Vs. Temperature $PO_2 = 0.1$ ATM Oxide B1 From ZrO_2 Gel Coated Powder	20
13. Estimated Ceria Electrolyte Performance	23
14. Estimated Ceria Electrolyte Performance	24
15. Estimated Ceria Electrolyte Performance	25



STATEMENT "A" per Dr. Robert Nowak
 ONR, Code 1113
 TELECON 2/7/90 CG

Accession For	
NTIS CRA&I	<input checked="" type="checkbox"/>
DTIC TAB	<input type="checkbox"/>
Unannounced	<input type="checkbox"/>
Justification	
By <i>per call</i>	
Distribution	
Availability Codes	
Dist	Avail and/or Special
A-1	

LIST OF TABLES

Table		Page
I	Electrical Properties Of Doped Ceria Electrolytes At 700°C	4
II	Electronic Properties Of Doubly Doped Ceria Effect Of Dopant Level 700°C	6
III	Bulk And Grain Boundary Conductivities 700°C, $PO_2 = 0.1$	14
IV	Electrical Properties Of Oxide B7 Made From $< 1\mu$ Ceria. 700°C	17
V	Electrical Properties Of Oxide B5 At 700°C	17
VI	Electrical Properties Of Oxide B1 Fabricated From ZrO_2 Coated Powders 700°C	19

SUMMARY

The primary obstacle to the use of ceria as a high power density solid oxide fuel cell electrolyte has been a low level electronic short. This develops under reducing (anode) conditions as a result of partial reduction of the CeO_2 lattice. The result is a decrease in:

- a) cell voltage,
- b) useful external current,
- c) efficiency,
- d) power density.

A dopant concept has been shown to lower the anode PO_2 below which the short becomes detrimental (electrolytic domain boundary) by two orders of magnitude. Two dopants, A and B have been shown to be effective. The optimum dopant A level was shown to be 1 - 3 metal atom percent. This reduction in the electronic short current is the primary achievement of this program.

Analysis of the activation energies for electronic and ionic conduction indicate that the dopant is effective in reducing the short by trapping the electronic charge carriers rather than preventing partial reduction of the ceria. Measurement of the grain boundary and bulk conductivities show the overall ionic conductivity is limited by grain boundary resistance. If lower grain boundary resistance can be achieved by processing changes, another two orders of magnitude improvement in electrolytic domain boundary is possible.

An attempt to limit the short by establishing an electronically resistive grain boundary barrier layer was abandoned. A separate grain boundary phase was difficult to maintain during the sinter densification step.

The dopant approach was selected for further development in Phase II.

INTRODUCTION

The high operating temperature of zirconia based solid oxide fuel cells has been shown in many studies to have advantages for both space and terrestrial applications. The high heat rejection temperature minimizes radiator size and weight for air and space applications. Mobile and stationary terrestrial applications take advantage of a cell temperature high enough to directly reform hydrocarbon fuels, achieving high efficiency and energy density.

Government funded solid oxide fuel cell (SOFC) efforts are concentrated on the monolithic and tubular cell designs employing zirconia as the oxide ion conduction membrane. Zirconia requires an operating temperature of 1000°C to achieve adequate electrolyte conductivity. All ceramic cell structures are used in both cases, leading to fragile, failure prone cells, and manufacturing steps which are difficult to scale up and costly. IFC's molten carbonate fuel cell development demonstrates the reliability of ductile sheet metal parts used for gas flow fields, separator plates, and frames in the 650°C temperature range. Ceria doped with gadolinia has ionic conductivity at 700°C comparable to zirconia at 1000°C . At 700°C a variety of stainless steels offer acceptable strength and oxidation resistance for use as cell hardware.

However a critical issue must be resolved if ceria is to be an ideal fuel cell electrolyte. When exposed to the reducing atmosphere at the fuel side, it develops electronic as well as ionic conductivity. This contributes to loss of efficiency at low power levels. This program addressed two means of ameliorating this loss. They were:

1. Modifying the ceria electronic structure through doping to enhance the ionic and diminish the electronic conductivity.

2. Incorporating non-electronically conducting barrier layers at the ceria grain boundaries to block electron flow.

Additional description for the rationale behind these approaches can be found in the First Interim Report for the Quarter Ending September, 1988, FCR-9983. During Phase I of this program, both approaches were pursued, and an optimum composition selected for further development in Phase II.

RESULTS

Task 1 Literature Search

A computer generated literature search was completed covering ceria and related topics for the years 1970 to the present. The pertinent references appear in the bibliography organized according to subject matter.

Task 2 Experimental Evaluation of Dopants to Increase the Ratio of Ionic to Electronic Conductivity

2.1 Sample Preparation and Electrical Measurement Techniques

Samples were prepared from 99.999 percent oxides by the mixed oxide technique during this report period. This change to high purity oxides was made in an effort to ensure reproducible and accurate results. The materials were purchased from Cerac. While believed to be too costly for practical fuel cell application, high purity minimizes the chance of measuring spurious results due to tramp dopants.

Weighed quantities of the oxides were ground in an agate mortar and pestle, calcined at 1000°C for 18 hours, and then reground. Pellets were pressed at 3636 Kg in a 1.85 cm pellet press using 2 w/o DOW XUS 40303 experimental binder. Sintering was accomplished in a Theta Furnace at 1600°C for 12 - 24 hours in air. A heat up rate of 2⁰/min and a cool down rate of 0.5⁰/min were used to minimize cracking. Sintered sample thickness was of the order of 2.5 mm.

Pt paste (Heraeus CL115100) contacts were applied and fired onto the faces of the sintered discs at 1000°C. Pt screen current collectors were attached with a second thin layer of Pt paste.

Samples were placed in an Inconel retort for electric property measurements as a function of oxygen partial pressure and temperature. The retort was fitted with gas inlet and exit ports, thermocouple wells, and electrical feed through and heated in a Sola Basic Lindberg furnace. The high PO₂ gas environments were provided by mixtures of O₂, N₂, and CO₂. The low PO₂ environments were established with H₂ and H₂ - N₂ mixtures passed through a water saturator set at 25° - 85°C. Measurements were taken at a high PO₂, (0.1 atm), then the lower PO₂s, and finally the high PO₂ was repeated to ensure no mechanical damage had occurred as a result of the partial reduction of the ceria. These experimental procedures led to stable, and reproducible data.

AC impedance analysis was used to separate electrode impedance from the impedance of the ceramic electrolyte. A Solatron 1250 Frequency Response Analyzer, and a 1286 electrochemical interface, both controlled by an IBM-XT computer with Z-Plot™ software was used to obtain the impedance spectra. At 700°C, the usual measurement temperature, the complex plane impedance plot generally showed the intersection of the low impedance end of the electrode impedance arc with the real axis. See for example Figure 1 taken from reference 4. This value was taken as the overall electrolyte impedance. Volume conductivity was calculated as usual from the geometric factors and corrected for porosity by the Bruggeman equation using a power of 1.5(1). At lower temperatures electrolyte bulk and grain boundary impedances could also be measured. At the lowest PO₂ levels the ionic impedance was essentially shorted by the electronic conduction and only a single point plot resulted.

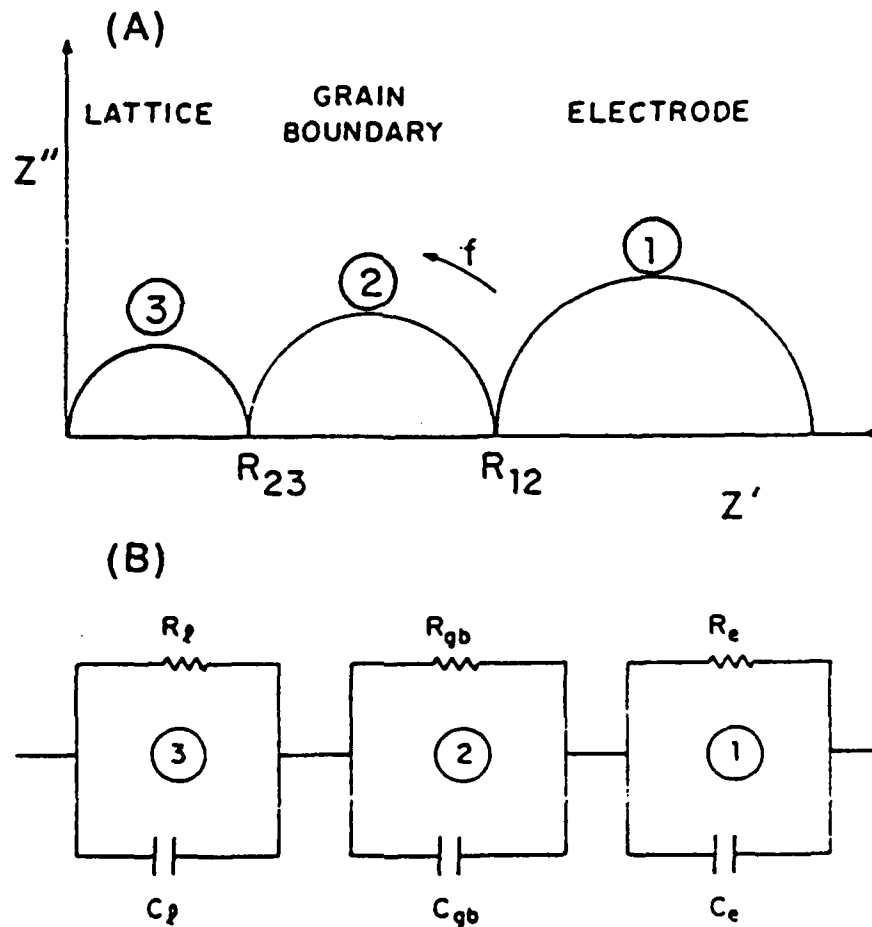


Figure 1. (A) Schematic diagram of a complex impedance plot showing arcs due to three processes. The arrow indicates the direction of increasing frequency. (B) The equivalent circuit that gives rise to the three arcs shown in (A).

2.2 Verification of Improved Electrolytic Domain Boundary by AC Impedance Analysis

Improvement in the level of electronic shorting induced in the ceria electrolyte under anode (reducing) conditions was assessed by measuring the electrolytic domain boundary (EDB). The EDB was determined by measuring the electrolyte impedance under gas compositions with a PO_2 ranging from 10^{-1} to 10^{-24} atm at $700^\circ C$ as described in section 2.1. The value of the volume conductivity calculated from the PO_2 10^{-1} atm data was assumed to be the ionic conductivity. The increase in volume conductivity observed as the PO_2 was lowered was taken as the electronic conductivity. This allowed calculation of the electronic conductivity at any PO_2 simply by subtracting the ionic conductivity from any increase in conductivity observed at low PO_2 (2). The electrolytic domain boundary was defined as the PO_2 at which the electronic and ionic conductivities are equal.

The improved experimental techniques described in section 2.1 were used in order to ensure steady reproducible conductivity measurements. A sample of $Ce_{0.8}Gd_{0.2}O_{2-Y}$ was measured with the same techniques as a reference point, and for comparison to EDB values from the literature.

Figure 2 illustrates the impact of dopant A on the total conductivity of the doped ceria electrolytes at $700^\circ C$. Based on this data, the ionic conductivity is enhanced, while the electronic conductivity is depressed. The net result is a reduction in the EDB of 2 orders of magnitude. This is illustrated in Table I. Measurements on each of two samples with and without 1 atom percent dopant A are compared with results calculated from data of Kudo and Obayashi(3) for Gd doped ceria. In this and following tables σ_{ion} refers to the ionic conductivity, σ_{el} to the electronic conductivity, and EDB to the electrolytic domain boundary.

TABLE I
ELECTRICAL PROPERTIES OF DOPE
CERIA ELECTROLYTES AT $700^\circ C$

Composition	σ_{ion}	σ_{el}	EDB
	$PO_2 = 0.1$ (S/cm)	$PO_2 = 10^{-23}$ (S/cm)	
Ce _{0.8} Gd _{0.2} O _{2-Y} - This study	2.8×10^{-2}	4.7×10^{-1}	3.5×10^{-19}
Ce _{0.8} Gd _{0.2} O _{2-Y} - This study	1.4×10^{-2}	1.8×10^{-1}	1.3×10^{-19}
Ce _{0.8} Gd _{0.2} O _{2-Y} - Ref (3)	4.7×10^{-2}	4.6×10^{-1}	1.24×10^{-19}
Oxide B1	3.7×10^{-2}	1.9×10^{-1}	4.6×10^{-21}
Oxide B1	4.2×10^{-2}	2.6×10^{-1}	4.7×10^{-21}

The reduction in EDB accomplished by dopant A is consistent and reproducible. The value of the ionic conductivity of Gd doped ceria is lower in this work than Kudo and Obayashi(3). This may reflect a different micro structure or level of impurities.

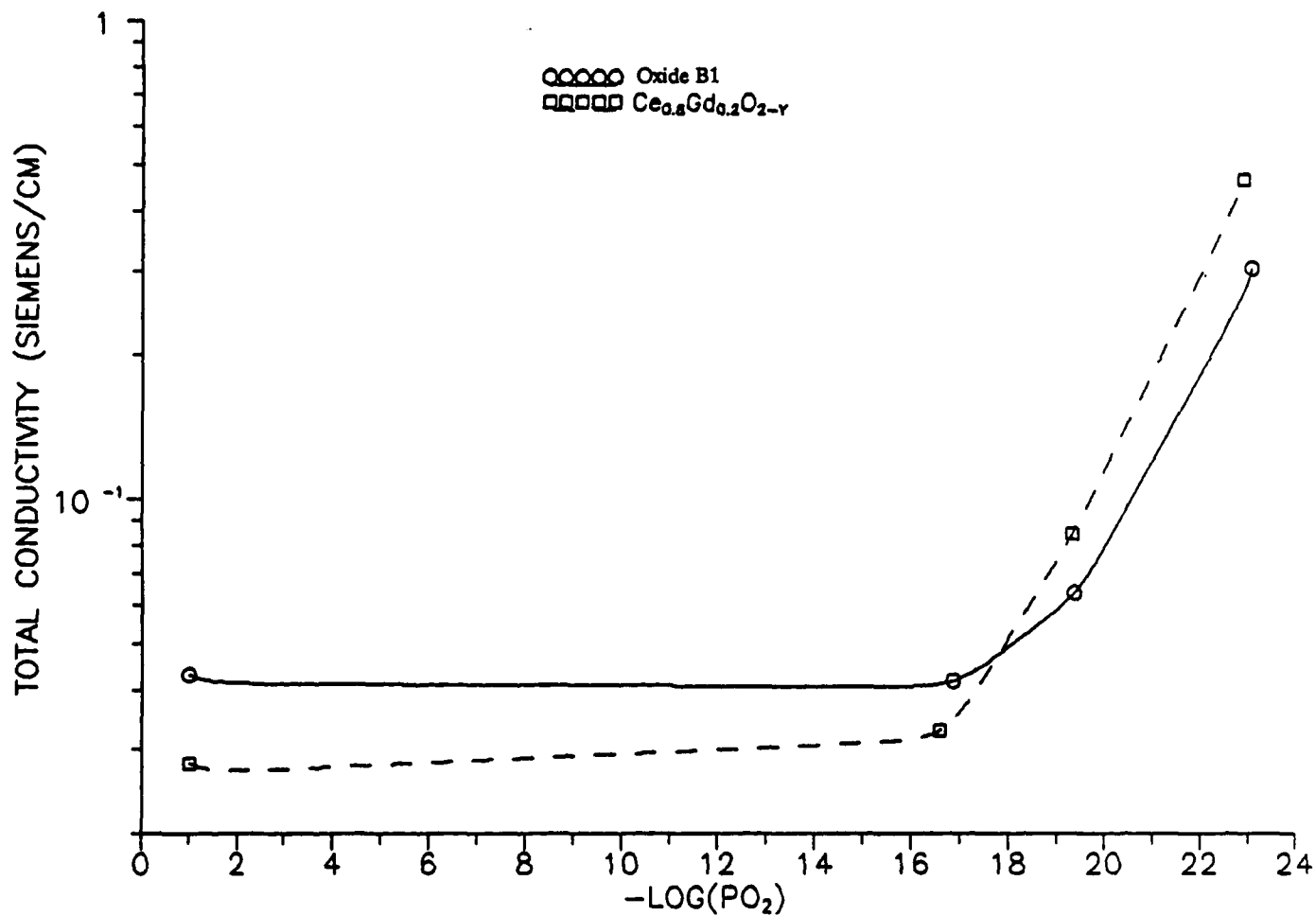


Figure 2. Total Conductivity as a Function of Oxygen Partial Pressure 700°C

2.3 Optimization of Composition

The one metal atom percent dopant A level used initially was selected on the basis of some early work which showed no benefit at the 5 to 20 percent level. However, it is necessary to determine the optimum level for the dopant. This was done by varying the dopant A level over the range of .01 to 6 metal atom percent. The compositions tested were: Oxide B4, Oxide B1, Oxide B3, and Oxide B6. The EDBs and the electronic conductivity at a PO_2 of 10^{-23} and $700^\circ C$ are shown in Figures 3 and 4. Both reach a broad minimum in the 1 - 3 metal atom percent range. This is the optimum composition for this dopant, and the data shown in section 2.2 represents near optimum electrical properties for these materials.

Table II shows the conductivity data obtained on these materials in tabular form. It is clear that the dopant A level has no impact on the ionic conductivity over the range of compositions studied. This suggests that the low ionic conductivity reported in section 2.2 for $Ce_{0.8}Gd_{0.2}O_{2-\gamma}$ in this study relative to Kudo and Obayashi(3) was likely due to poor micro structure, and that the effect of dopant A is primarily to lower the electronic conductivity.

TABLE II
ELECTRONIC PROPERTIES OF DOUBLY DOPED CERIA
EFFECT OF DOPANT LEVEL
700°C

Composition	Dopant A Level (metal atom%)	σ_{ion} $PO_2 = 0.1$ (S/cm)	σ_{el} $PO_2 = 10^{-2}$ (S/cm)	EDB (atm)
Oxide B4	0.1	4.2×10^{-2}	2.7×10^{-1}	7.5×10^{-21}
Oxide B1	1.0	3.7×10^{-2}	1.9×10^{-1}	4.6×10^{-21}
Oxide B3	3.0	4.3×10^{-2}	2.0×10^{-1}	1.1×10^{-21}
Oxide B6	6.0	3.5×10^{-2}	2.3×10^{-1}	3.5×10^{-21}

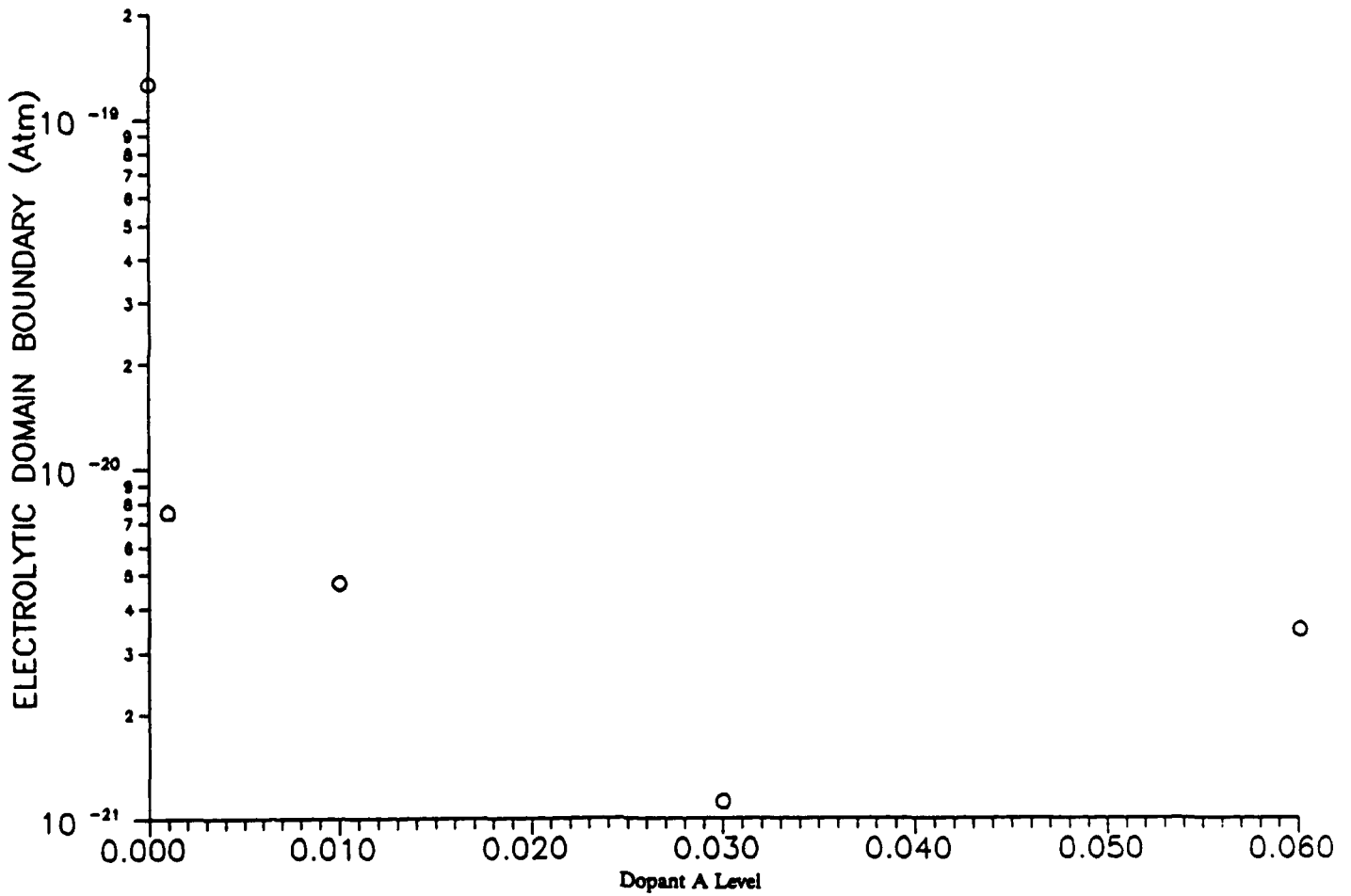


Figure 3. Electrolytic Domain Boundary Vs. Dopant A Level at 700°C

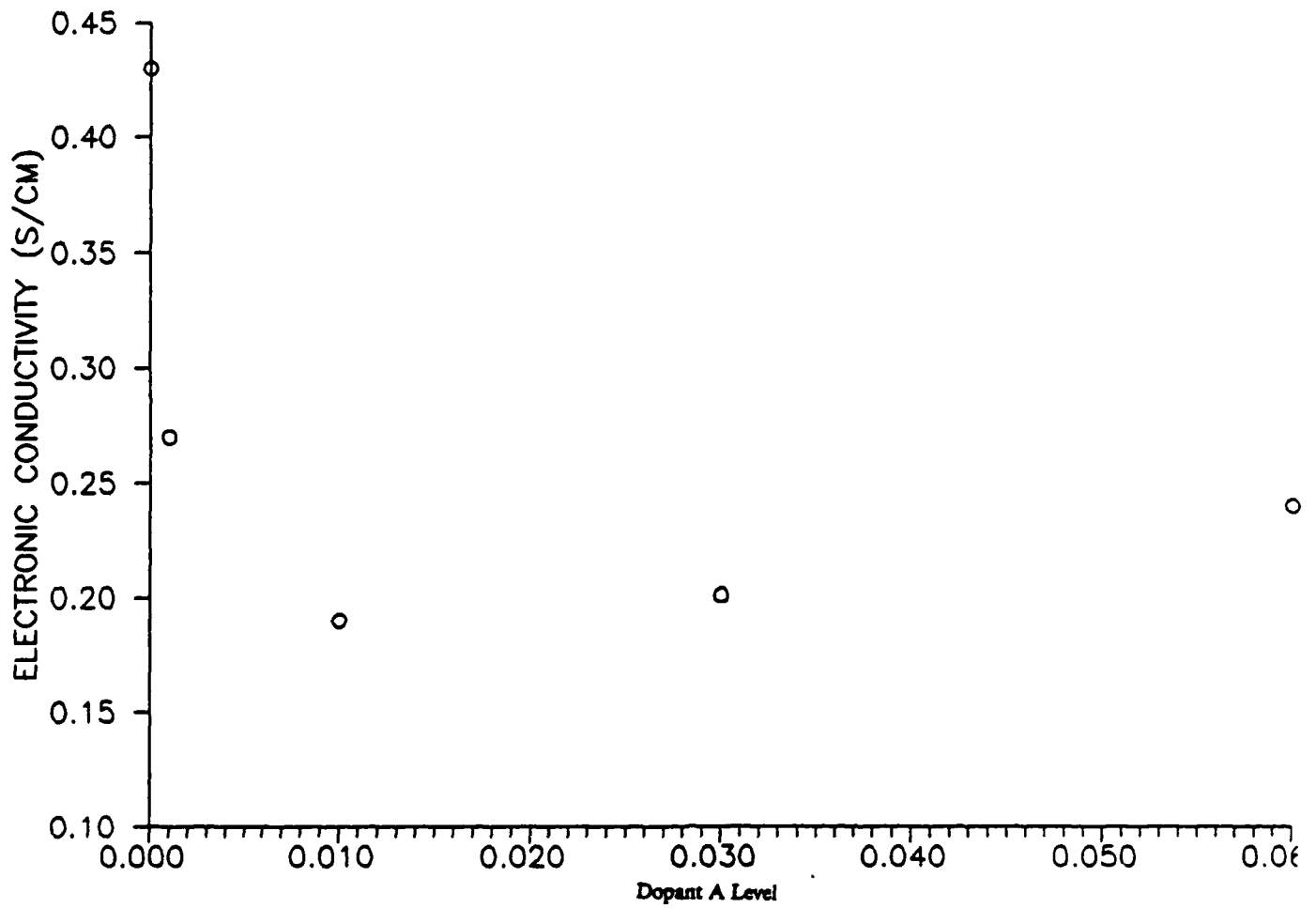


Figure 4. Electronic Conductivity at $PO_2 = 10^{-23}$ Vs. Dopant A Level

2.4 Measurement of Activation Energy of Electronic and Ionic Conductivity

Measurement of the behavior of electronic and ionic conductivity as a function of temperature was undertaken for two important reasons, one practical and one theoretical. No high power density fuel cell can be operated as an isothermal device due to waste heat rejection requirements. Therefore quantitative prediction of the effect of temperature on conductivity (power density), and on the EDB (efficiency) is required to assess the useful operating temperature range of this new fuel cell electrolyte. Secondly, analysis of the change in the electronic conductivity with temperature can help us understand the mechanism by which the dopant lowers the EDB.

The activation energy of the ionic conduction (E_i) was determined by measuring the conductivity at a PO_2 of 0.1 atm and plotting σT vs $10^3/T$, (σ = conductivity). The plot for Oxide B3 is shown in Figure 5. The slope yields an activation energy of 0.73 eV. This is in good agreement with the value of 0.69 eV calculated for $Ce_{0.8}Gd_{0.2}O_{2-y}$ from the data in Figure 6 of reference (3). This indicates that the dopant is not altering the conduction of O^\ominus in the ceria lattice.

The impact of temperature on electronic conductivity was determined by measuring the total conductivity as a function of PO_2 at three temperatures. The ionic conductivity was then subtracted to yield σ_{el} vs PO_2 at the three temperatures. This data is shown in Figure 6. Best fit lines of slope = $-1/4$ were drawn through the data at each temperature. Extrapolation to $PO_2 = 10^{-18}$ yielded σ_{el} as a function of temperature at a fixed PO_2 . This data plotted as σT vs $10^3/T$ is shown in Figure 7, and yields an activation energy of 2.18 eV.

As pointed out by Kudo and Obayashi(3), this activation energy includes the enthalpy of reduction of the ceria lattice to generate the electrons as well as the activation energy for the mobility of the electrons (E_e). However, since $E_e \ll E_i$, and $E_i = 0.73$ eV, the measured activation energy is dominated by the enthalpy of reduction term. In fact, if one calculates the enthalpy of reduction per electron from Figure 7 of reference (3) for the composition $Ce_{0.8}Gd_{0.2}O_{2-y}$ one obtains a very similar value of 2.17 eV. This indicates that dopant A has not stabilized the ceria lattice against reduction, but more likely has reduced the number of electronic carriers by trapping electrons in agreement with the original hypotheses.

The data in Figure 6 also yields EDB vs temperature by noting the PO_2 at which the electronic conductivity intersects the ionic conductivity value (marked by cross bars in Figure 6). Figure 8 shows the EDB plotted vs $10^3/T$ for Oxide B3 from this work, and compares it to $Ce_{0.8}Gd_{0.2}O_{2-y}$ from reference (3). This illustrates that the nearly two orders of magnitude improvement in EDB holds over the whole temperature range of interest to fuel cells. The value of the EDB at 700°C taken from the least squares fit of this data is 3.7×10^{-21} for Oxide B3 vs 1.24×10^{-19} for $Ce_{0.8}Gd_{0.2}O_{2-y}$ from the data of Kudo and Obayashi (3).

Figure 8 also provides insight into the upper temperature limit for useful fuel cell operation. Higher temperatures improve power density, but limit efficiency due to the increasing EDB. This data will be useful in predicting ceria cell performance as a function of temperature and fuel composition.

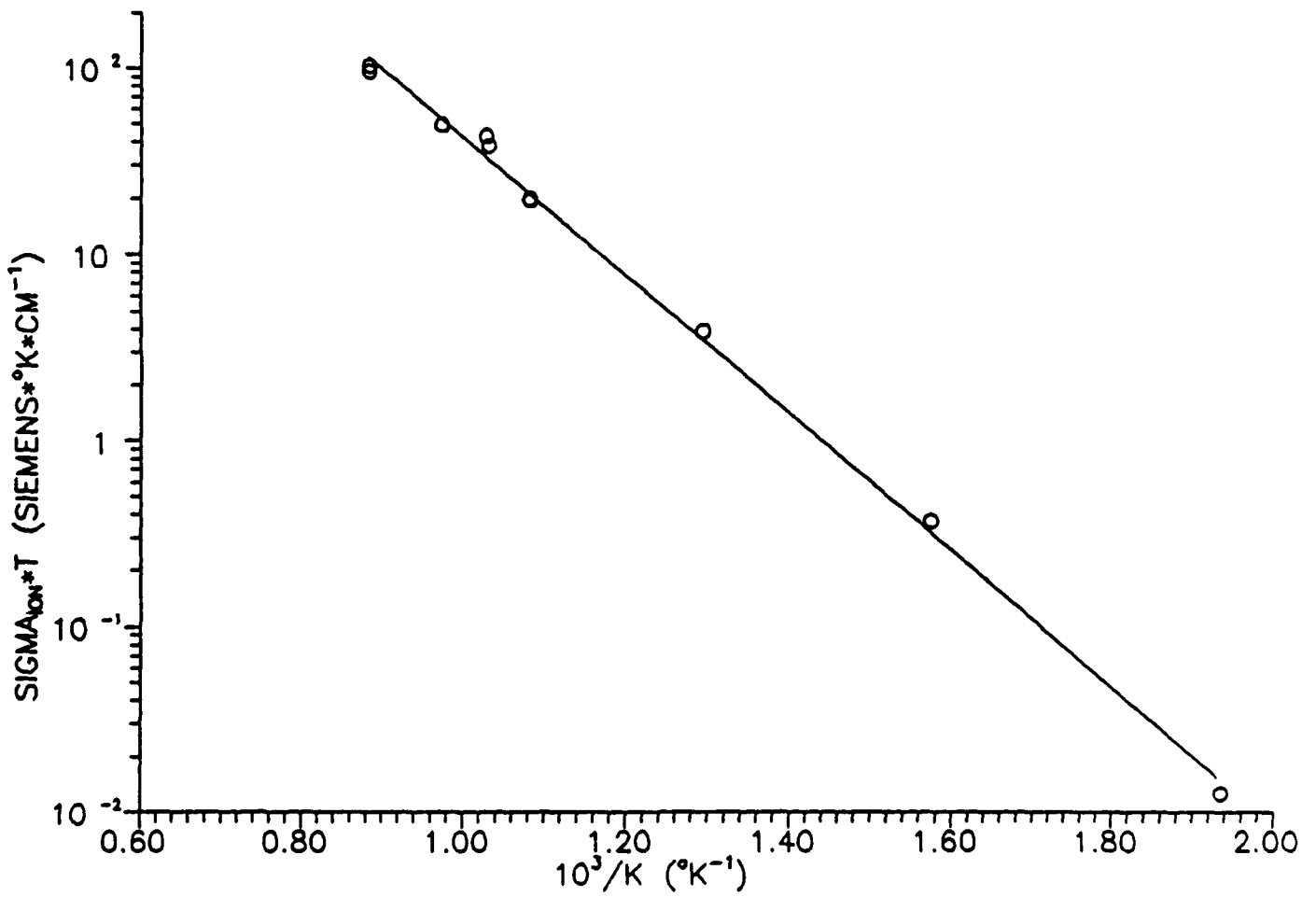


Figure 5. Ionic Conductivity - Temperature Behavior
Oxide B3 at $PO_2 = 10^{-1}$

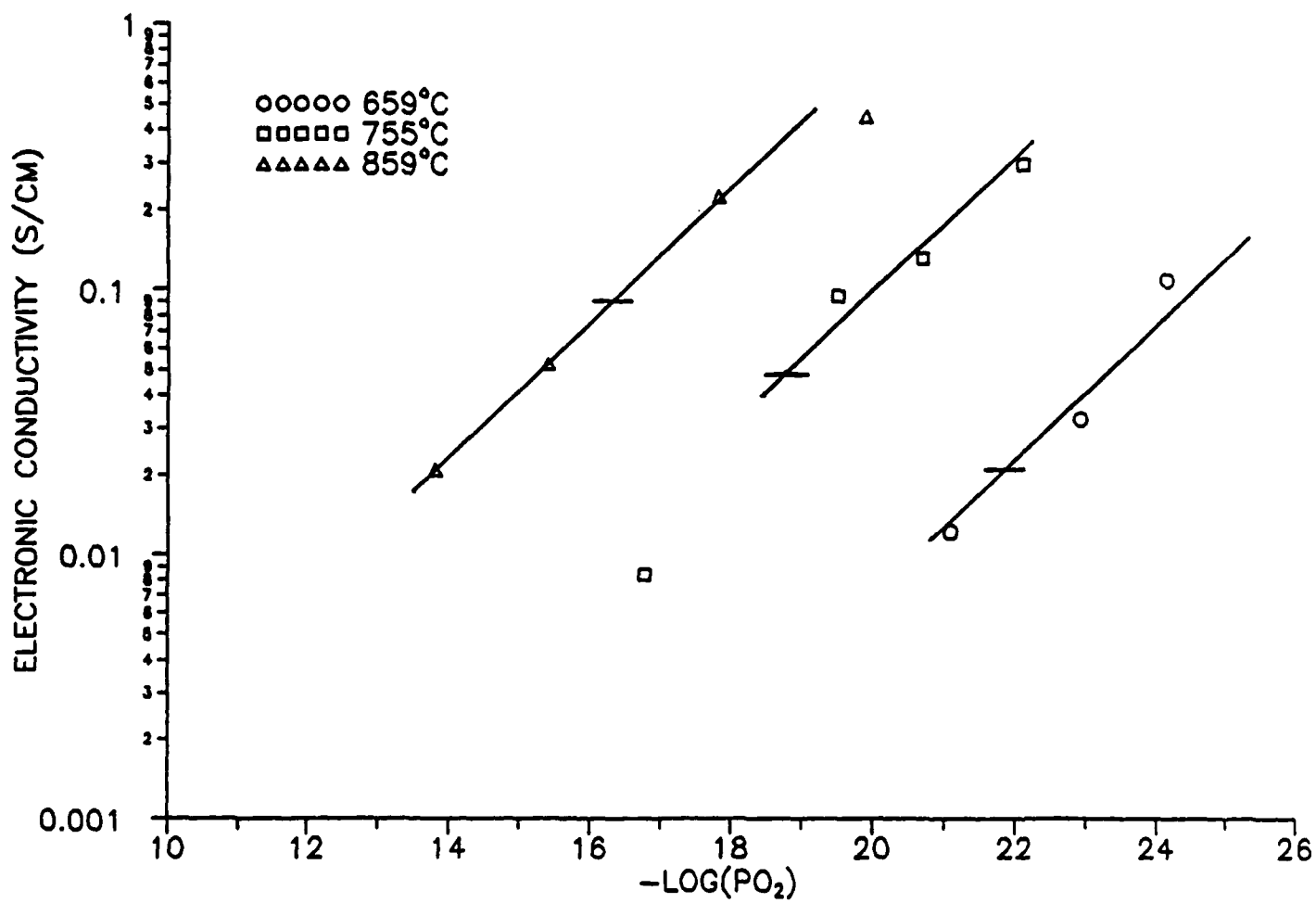


Figure 6. Electric Conductivity Vs. PO₂ at 3 Temperatures Oxide B3

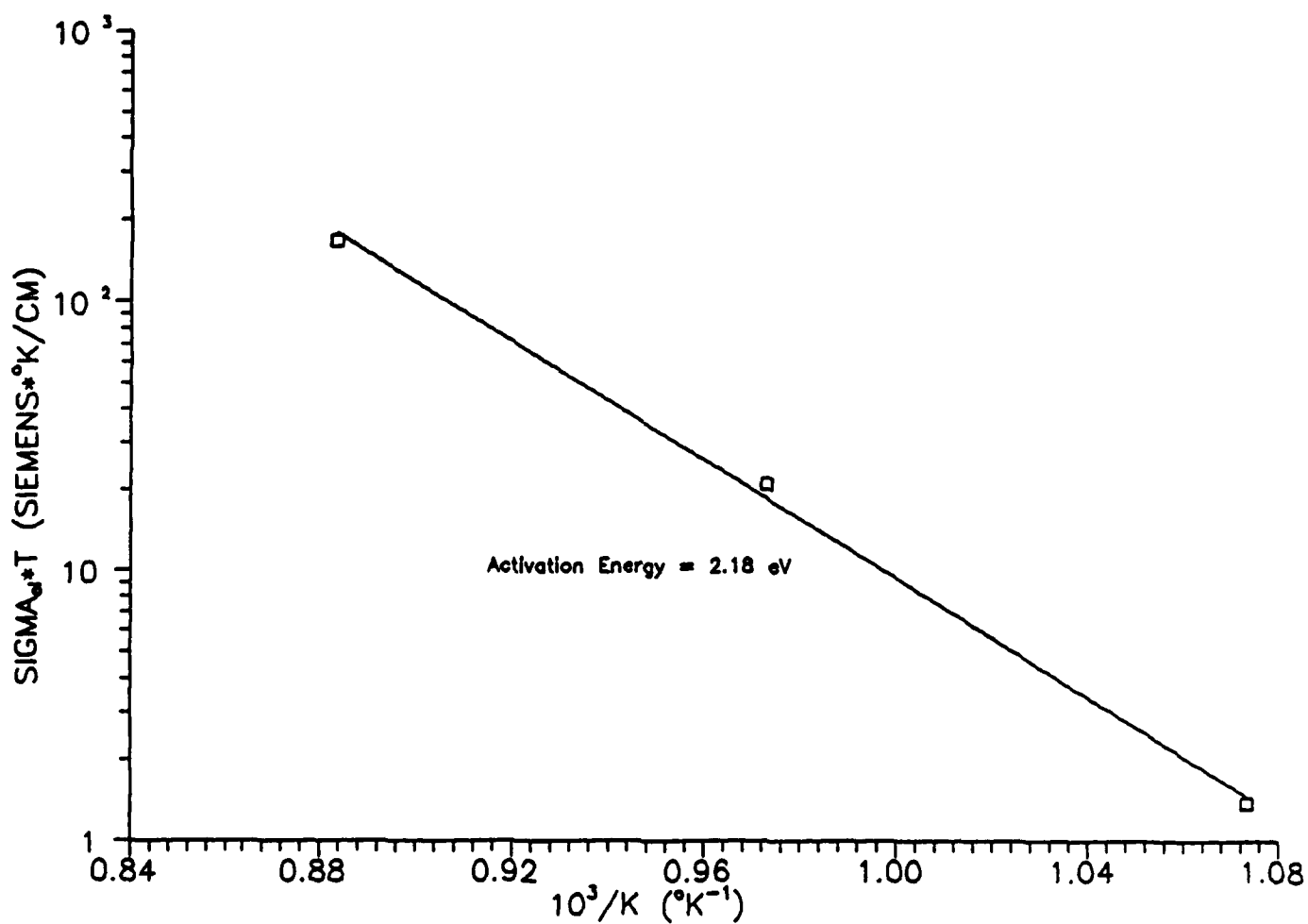


Figure 7. Electronic Conductivity - Temperature Behavior Oxide B3 at PO₂ = 10⁻¹⁸

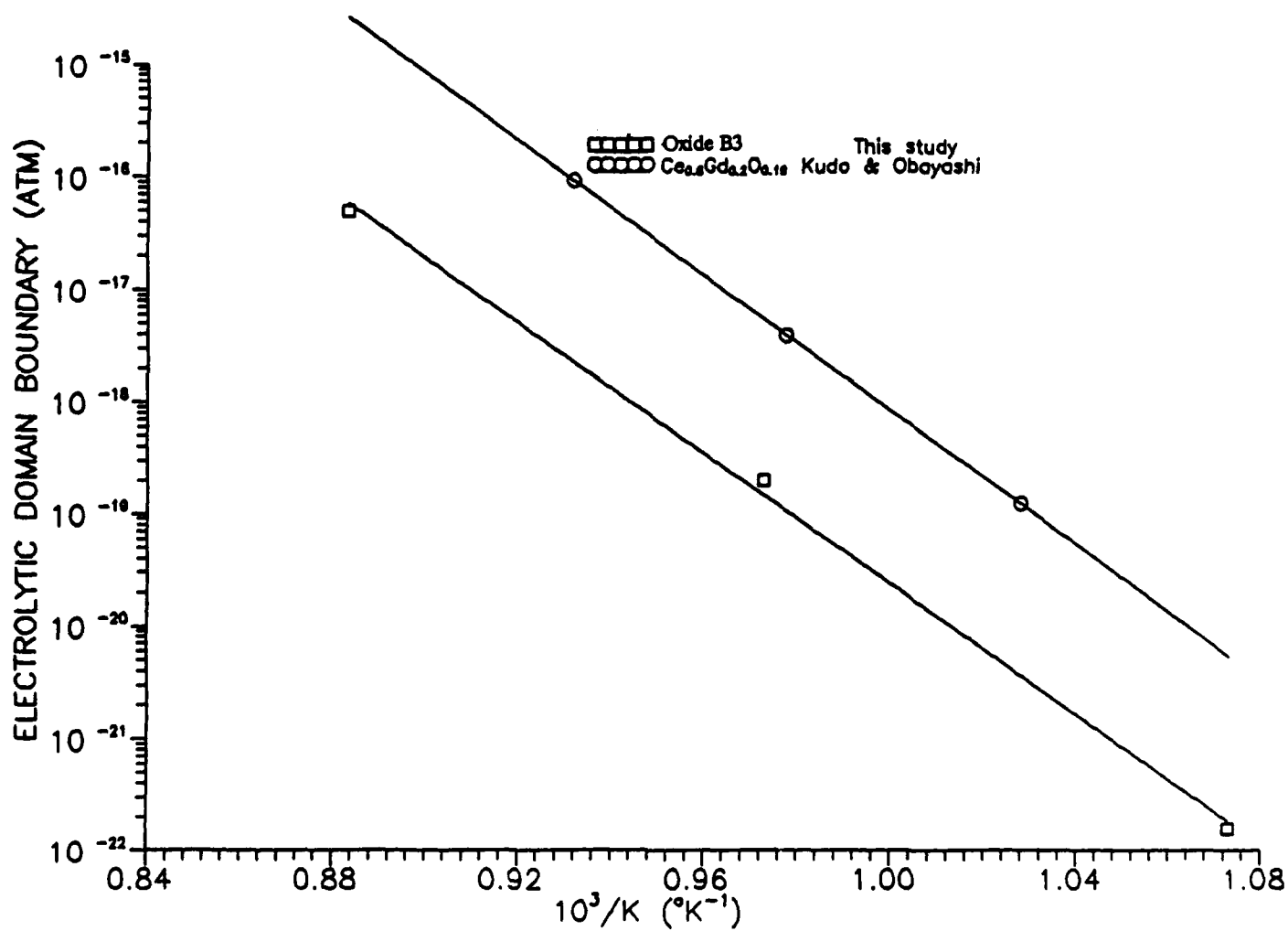


Figure 8. Temperature Behavior of Electrolytic Domain Boundary

2.5 Analysis of Bulk and Grain Boundary Conductivities as a Function of Temperature

A major advantage of using AC impedance analysis for the study of solid state electrolytes is the opportunity to separate grain boundary from bulk resistances. An operating fuel cell must contend with both sources of polarization losses, however, understanding the fundamental causes often leads to opportunities for engineering the material to optimize performance. In this case the bulk conductivity is a basic material property, but the grain boundary conductivity is determined by micro-structure and grain boundary chemistry (4). These are influenced primarily by processing parameters and are therefore amenable to improvement by changes in processing technique. Separation of these two sources of iR losses is important in order to assess how much more improvement in the electrical properties of the doped ceria might be possible.

Increasing the ionic conductivity has a dual benefit. It improves the potential power density at a given electrolyte thickness, and at a fixed electronic conductivity vs PO_2 relationship, it lowers the EDB, improving efficiency. This provides strong incentive for determining if grain boundary resistance contributes substantially to overall electrolyte resistance.

In order to separate the grain boundary from the bulk impedance within the frequency range available from the Solartron 1250 FRA, it was necessary to lower the temperature well below $700^\circ C$. At temperatures in the $200 - 300^\circ C$ range, two additional arcs are seen on the complex plane impedance plot (see Figure 2). Both lie between the lower end of the electrode curve and 0 on the real axis. The intersection of the upper end of the lowest arc on the real axis is assigned to the bulk, or lattice resistance, while the width of the intermediate arc on the real axis measures the grain boundary resistance (4)(5).

This technique was used to measure the bulk and grain boundary conductivities of several dopant A ceria samples as a function of temperature. For reference $Ce_{0.8}Gd_{0.2}O_{2-\gamma}$ was also included. Figure 9 shows an example of conductivity plotted vs. $10^3/T$ for $Ce_{0.8}Gd_{0.2}O_{2-\gamma}$. Table III presents the bulk and grain boundary conductivities extrapolated to $700^\circ C$ and the activation energies deduced from plots of σT vs $10^3/T$. Figure 10 illustrates this type of plot for Oxide B1.

TABLE III
BULK AND GRAIN BOUNDARY CONDUCTIVITIES
 $700^\circ C, PO_2 = 0.1$

Compound	σ_{Bulk} (S/cm)	σ_{Gb} (S/cm)	E_{Bulk} eV	E_{Gb} eV
$Ce_{0.8}Gd_{0.2}O_{2-\gamma}$	1.5×10^{-1}	9.9×10^{-2}	1.05	1.16
Oxide B1	1.4×10^{-1}	6.9×10^{-2}	0.92	1.02
Oxide B3	3.4×10^{-1}	*	0.90	*
Oxide B6	1.04×10^{-1}	9.9×10^{-1}	0.80	0.98

* Insufficient data

Inspection of the data in Table III reveals that the bulk conductivity of the B type samples is approximately twice the grain boundary conductivity. This means the grain boundary resistance is limiting the overall ionic conductivity, and substantial gains in ionic conductivity, and reduction of the EDB should result when the micro-structure is improved to minimize grain boundary resistance.

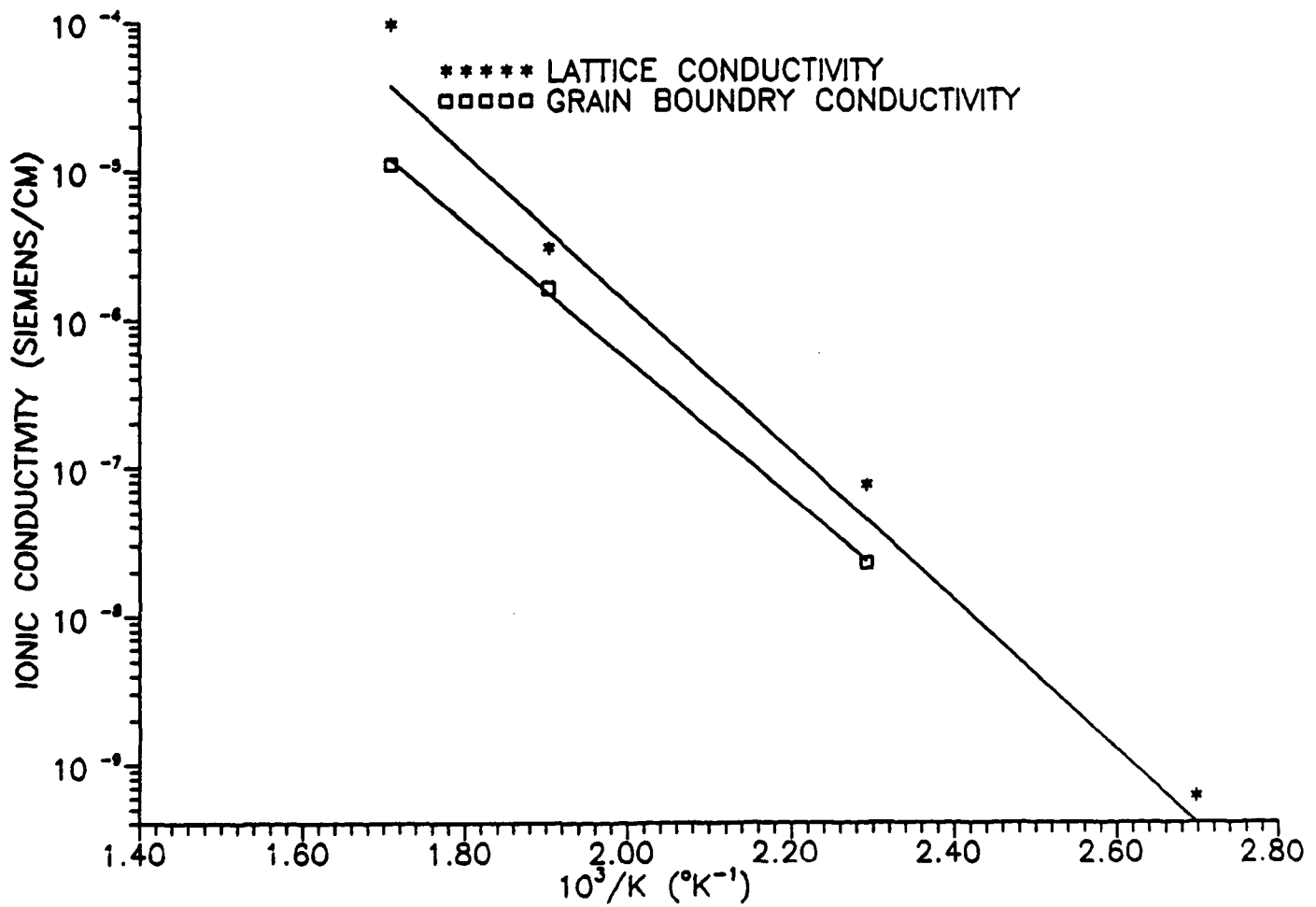


Figure 9. Conductivity Vs. Temperature, $PO_2 = 0.1$
 $Ce_{0.8}Gd_{0.2}O_{2-\gamma}$

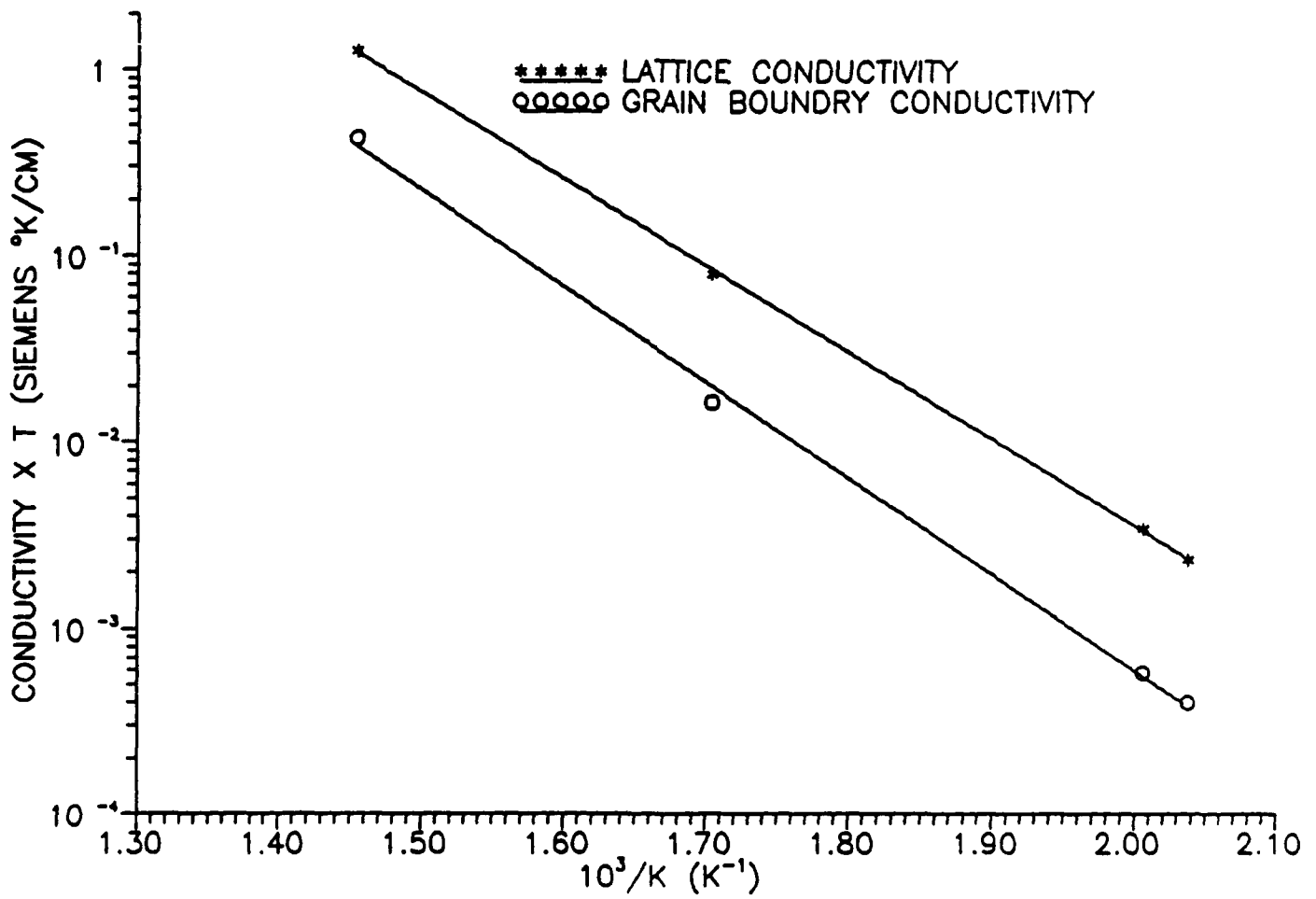


Figure 10. Conductivity *T Vs. Temperature, $PO_2 = 0.1$
 Oxide B1

2.6 Impact of Grain Size on Electronic and Ionic Conductivity

In order to use ceria as a practical fuel cell electrolyte, a density high enough to ensure no reactant cross leakage is required. Densities of the samples tested up to this point in the program ranged from 85–90 percent of theoretical. This is not high enough to ensure no through porosity. One approach to improving density is to use a high surface area, and therefore more sinterable starting material. This was accomplished by starting the mixed oxide synthesis with Opaline, a naturally occurring ceria available from Rhone Poulenc. This material has a relatively uniform particle size which lies mostly below 1μ

Discs prepared from Opaline did achieve an increase in density, to 93 percent of theoretical. However, when the electrical properties were measured this was found to be at the expense of ionic conductivity. The data is shown in Table IV.

TABLE IV
ELECTRICAL PROPERTIES OF OXIDE B7 MADE FROM $<1\mu$ CERIA. 700°C

σ_{ion} $\text{PO}_2 = 0.1$ (S/cm)	σ_{el} $\text{PO}_2 = 10^{-23}$ (S/cm)	EDB (atm)
2.5×10^{-2}	1.14×10^{-1}	4.5×10^{-21}

Both the ionic and electronic conductivities are lower by a factor of 2 than the data for Oxide B7 made from the 99.999 percent oxides with larger particle size. The smaller grain size which led to higher density also reduced the conductivities. Although the EDB is unchanged, the lower conductivity would adversely affect the potential fuel cell power density. This approach to improving density was not pursued.

2.7 New Compositions

It is of interest to know whether dopant A is the only or even the most effective dopant. Other elements have similar properties and might perform the same function. Dopant B is a candidate. A sample of Oxide B5 was prepared and subjected to electrical evaluation. The data shown in Table V illustrates that dopant B produces the same reduction in EDB as dopant A.

TABLE V
ELECTRICAL PROPERTIES OF OXIDE B5 AT 700°C

σ_{ion} $\text{PO}_2 = 0.1$ (S/cm)	σ_{el} $\text{PO}_2 = 10^{-23}$ (S/cm)	EDB (atm)	σ_{Bulk} $\text{PO}_2 = 0.1$ (S/cm)	σ_{Gb} $\text{PO}_2 = 0.1$ (S/cm)
4.3×10^{-2}	1.7×10^{-1}	2.6×10^{-21}	1.88×10^{-1}	4.8×10^{-2}

Figure 11 shows the bulk, and grain boundary conductivities plotted vs temperature. The activation energies obtained from the σT plots were 0.94 eV and 0.93 eV for the lattice and grain boundary conductivities respectively.

A similar possibility is to use dopant B and dopant A. This combination was also explored briefly. total conductivity vs PO_2 was measured for the composition Oxide A1. The ionic conductivity was 3.7×10^{-2} , and the EDB 6×10^{-24} , at 700°C . These values are identical and slightly higher respectively than the results for Oxide B1 shown in Table I. It broadens the scope of the dopant concept, but provides no incentive to switch to dopant B as the primary dopant.

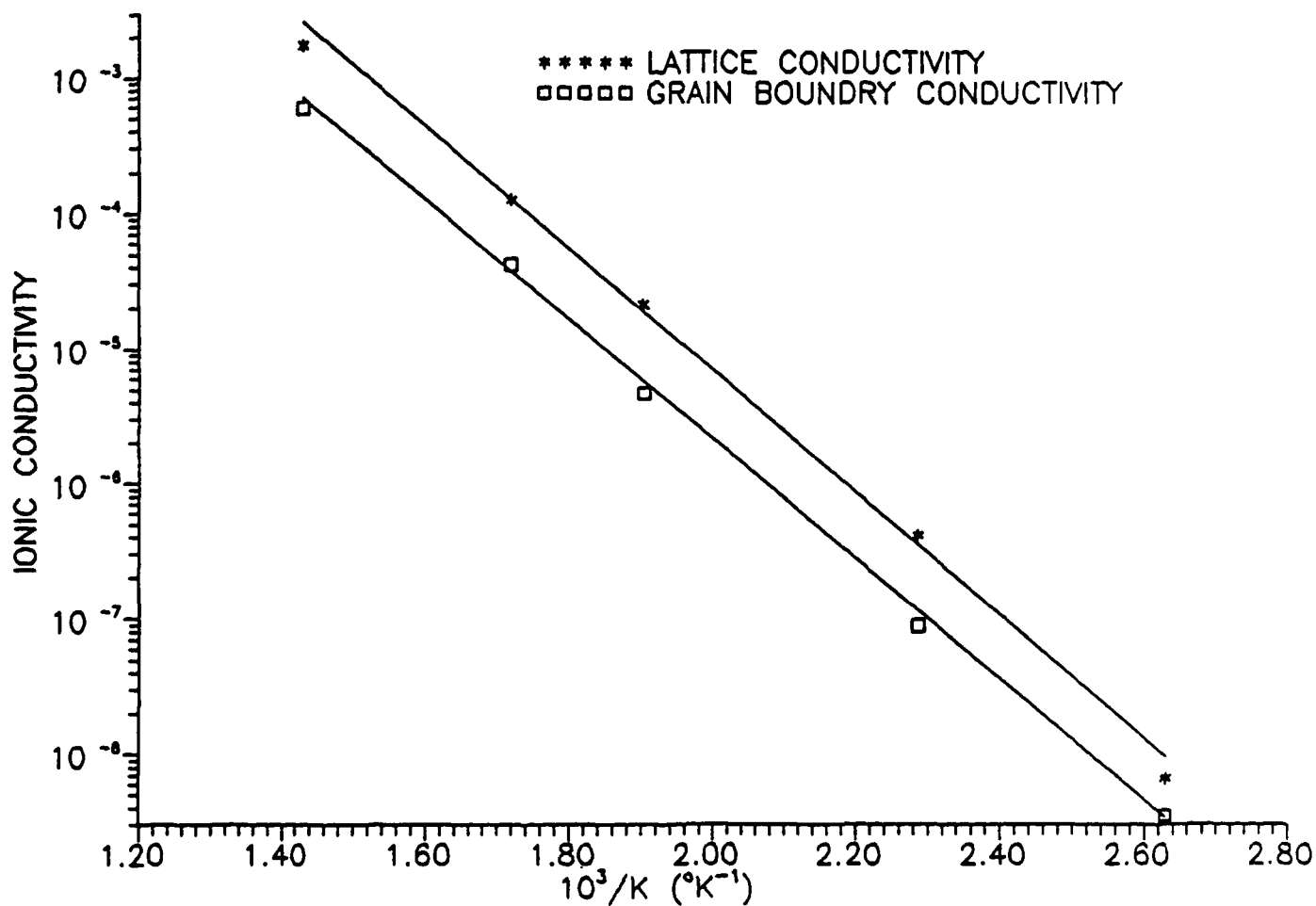


Figure 11. Conductivity Vs. Temperature, $PO_2 = 0.1$
 Oxide B5

Task 3 Experimental Evaluation of Barrier Layers to Increase the Ratio of Ionic to Electronic Conductivity

3.1 Evaluation of Zirconia as Grain Boundary Barrier Layer.

Task 3 of this program proposed an alternative approach for lowering the EDB of ceria based electrolytes. This "barrier layer" concept involved introducing a grain boundary phase which had as high as possible ionic conductivity at 700°C, but no appreciable electronic conductivity. This was viewed as a fall-back approach due to an expected ionic conductivity penalty.

A single attempt was made to test this concept based on a gel coating process developed by Prof. Samantha Amarakoon of Alfred University (6)(7). A sample of Oxide B1 powder was sent to Alfred University, where it was gel coated with yttria stabilized zirconia. The process for producing the gel coated powder is described in a report by Prof. Amarakoon which is attached as Appendix A.

The two phase powder with an electronically insulating zirconia coating around a core of doped ceria was analyzed at IFC revealing a ZrO₂ level of 1.3 wt percent. This material was then processed into a disc as described in Section 2.1. No changes were made in the sinter cycle since densities were already low. The plan was to leave the ZrO₂ as a grain boundary phase, providing a barrier to electronic conduction. Electrical properties are shown in Table VI.

TABLE VI
ELECTRICAL PROPERTIES OF OXIDE B1
FABRICATED FROM ZrO₂ COATED POWDERS
700°C

σ_{ion} PO ₂ = 0.1 (S/cm)	σ_{el} PO ₂ = 10 ⁻²³ (S/cm)	EDB (atm)	σ_{Bulk} PO ₂ = 0.1 (S/cm)	σ_{Gb} PO ₂ = 0.1 (S/cm)
3.0x10 ⁻²	1.62x10 ⁻¹	1.1x10 ⁻²⁰	7.8x10 ⁻²	1.15x10 ⁻¹

Comparison of this data with Table III reveals that the net result of adding the ZrO₂ was to lower the ionic conductivity while leaving the electronic conductivity almost the same. This raised the EDB, the opposite of the desired result.

Figure 12 shows the grain boundary and bulk conductivities vs temperature data for this sample. The extrapolated 700°C conductivities (Table VI) compared to the uncoated sample of the same composition (Table III) show lower bulk conductivity and higher grain boundary conductivity. This is just the reverse of the expected result if the ZrO₂ were a grain boundary phase. The implication is that the Zr diffused into the ceria during the sinter cycle, lowering the bulk ionic conductivity.

A sintered sample was returned to Alfred University for verification of this conclusion by transmission electron microscopy. The results reported in Appendix A concur with the electrical measurements. Zirconia was found throughout the polycrystalline ceramic rather than concentrated in the grain boundary regions.

The ZrO₂ did however perform the roll of a sintering aid. This led to a high density (93% of theoretical) which presumably helped improve the grain boundary conductivity. The activation energies from σT vs 10³/T analysis were 0.98 eV, and 0.88 eV for grain boundary and bulk conductivities, respectively.

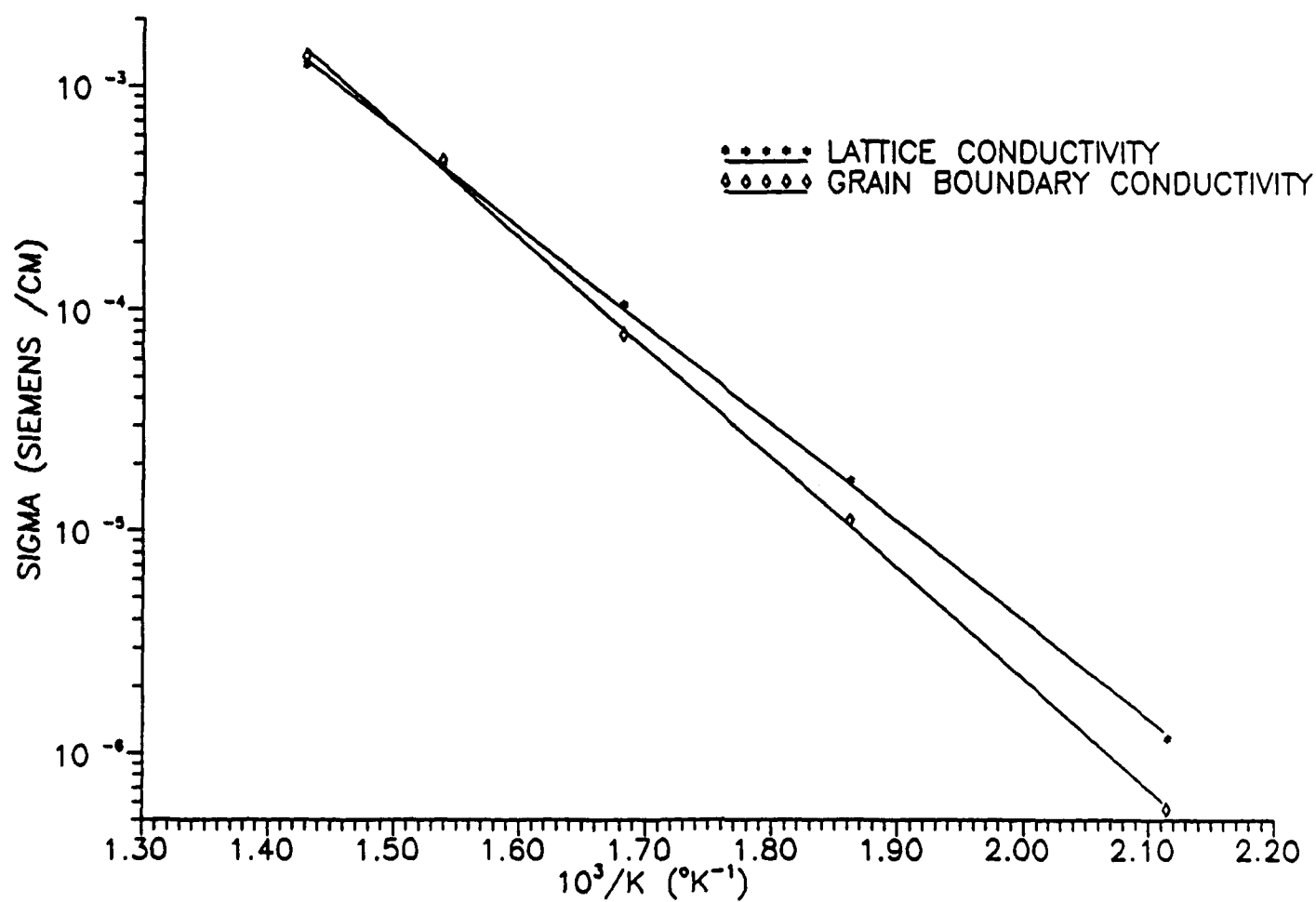


Figure 12. Conductivity Vs. Temperature $PO_2 = 0.1$
ATM Oxide B1 From ZrO_2 Gel Coated Powder

On the basis of this experience, the doping concept, rather than the barrier layer, was selected as the preferred approach. This decision reflected primarily the perceived difficulty of achieving phase separation and density at the same time with a practical fabrication process.

Phase I Program Review

A. Recommended Approach

The most promising approach to reducing the electronic conductivity of CeO_2 electrolytes has been identified as modifying the composition to trap the electrons produced by partial reduction of the ceria under anode conditions. This approach forms the basis of a Phase II program plan presented in Appendix B. This program finishes the development of the electrolyte and develops anode and cathode materials and application process. The plan continues development of a ceria electrolyte fuel cell system capable of high power density operation. It culminates with demonstration of the technology at the 1 kW level

B. Calculated Cell Performance Parameters

The data presented in Task 2 has been expressed in terms of fundamental electrical properties of the ceramic ceria electrolyte. In order to assess the significance of the improvements made to fuel cell operation, the model developed at UTC(8) was used to illustrate the improvement in fuel cell operating parameters.

Since no electrodes have been specifically developed for ceria electrolytes, and this program is concerned with electrolyte properties only, electrode losses were not considered (assumed = 0). An anode PO_2 of 4×10^{-22} atm, simulating a reformed hydrogen fuel at 700°C , was assumed. The electronic properties of $\text{Ce}_{0.8}\text{Gd}_{0.2}\text{O}_{2-\gamma}$, and Oxide B1 were taken from this work, Table I, Task 2.2.

Figure 13 illustrates the calculated performance improvement for Oxide B1 relative to $\text{Ce}_{0.8}\text{Gd}_{0.2}\text{O}_{2-\gamma}$ in terms of the usual current voltage plot. The higher performance for the former is primarily due to the higher ionic conductivity measured for the dopant A doped material. At low current densities the lower electrolytic domain boundary also contributes to higher performance for the Oxide B1 material.

Also plotted is the calculated electronic short current. This is reduced by a factor of two at low current densities as a result of the lowered EDB for the dopant A material. The short current is a steep non linear function of cell voltage (and therefor current density). As the cell polarizes, the PO_2 at the surface of the anode rises, lowering the electronic conductivity (raising the ionic transference number). At the same time the driving voltage across the electronic conductance also decreases. The combined influence of these effects is responsible for the rapid drop off in electronic short current as the cell voltage is lowered by increasing the current density. This reduction in the electronic short current is the primary achievement of this program.

Figure 14 shows the calculated thermal cell efficiency for both materials plotted on the same standard current voltage curve. The thermal cell efficiency is defined as the dc power out of the cell over the higher heating value of the fuel consumed electrochemically. The peak thermal cell efficiency has been improved from 40 to 48 percent by the new dopant. This curve also illustrates that the only real impact of the electronic short on fuel cell performance is reduced efficiency at low power. At a typical design voltage, say 0.6 volts, the efficiency is controlled almost exclusively by the resistive losses as with any other solid electrolyte fuel cell.

Figure 15 overlays a cell power output curve (electrode losses assumed = 0) on the voltage and efficiency plots for Oxide B1. This plot illustrates that the fall off in efficiency at low power does not become

extreme until the cell power output falls below 1/3 of peak. For example peak power at 0.6 volts/cell and 2 A/cm² is 1.2 w/cm². At 0.4 w/cm² the efficiency is still 40 percent. On the basis of cell consideration alone, this provides a 3:1 turndown ratio with in the range of reasonable fuel cell efficiencies.

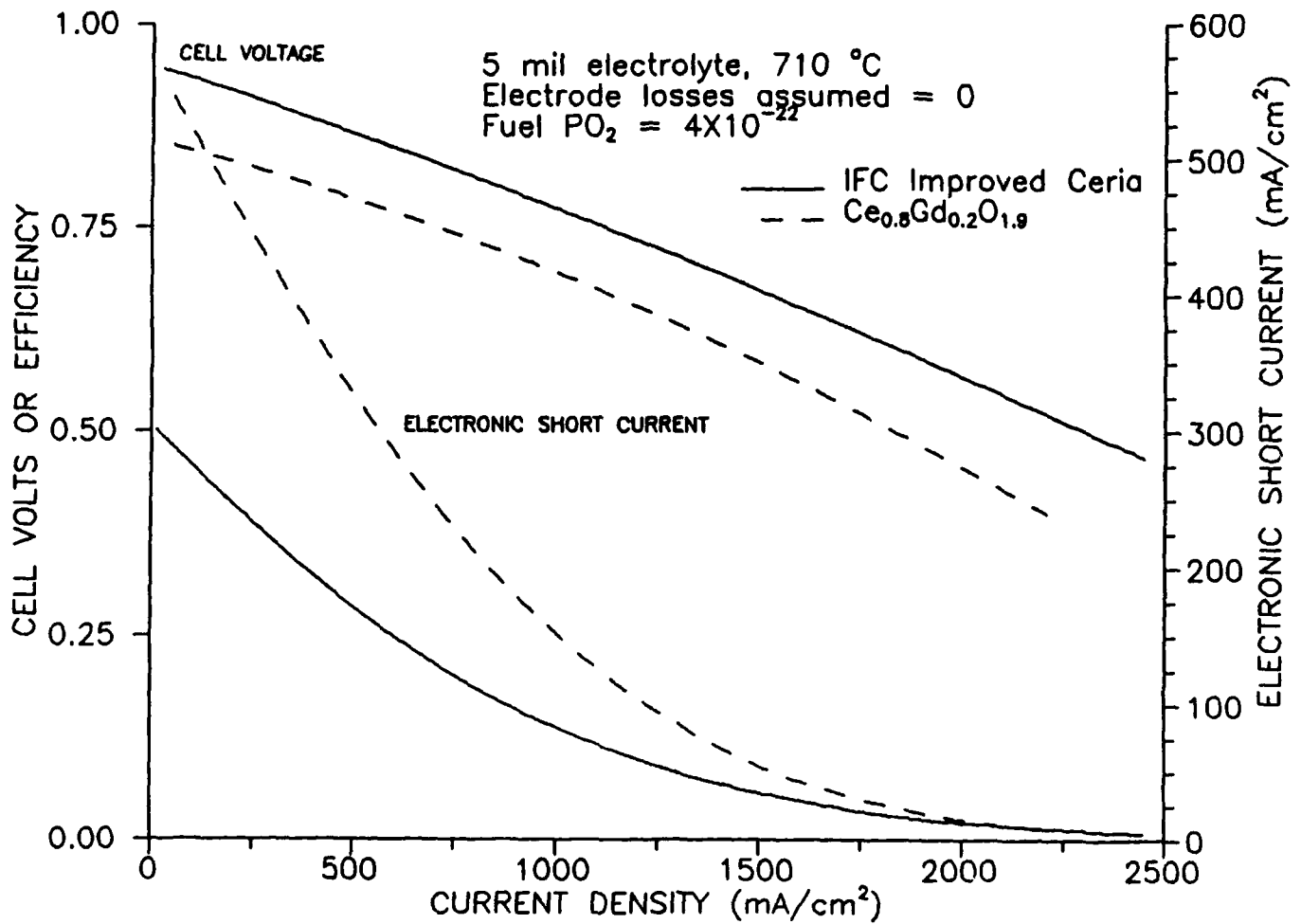


Figure 13. Estimated Ceria Electrolyte Performance

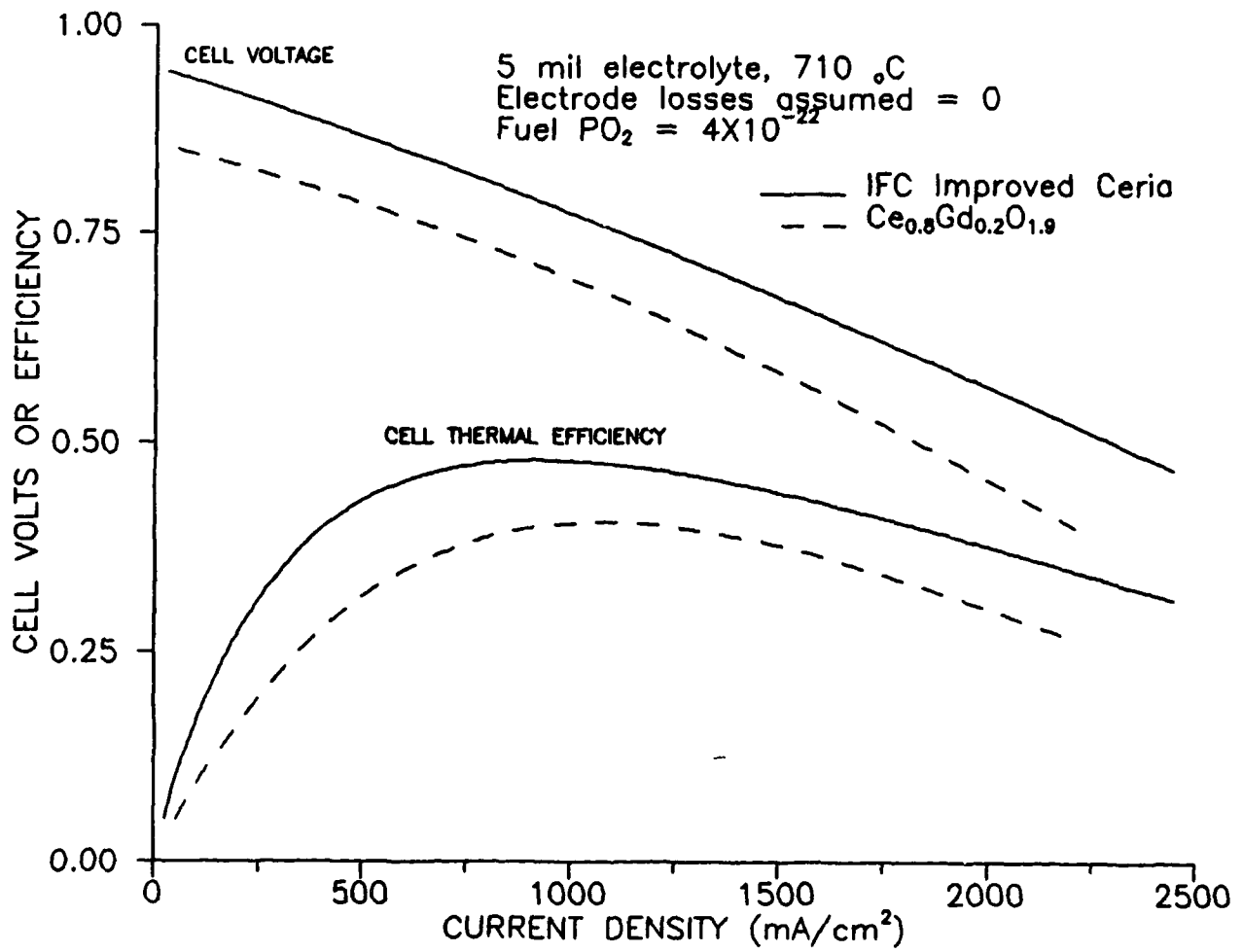


Figure 14. Estimated Ceria Electrolyte Performance

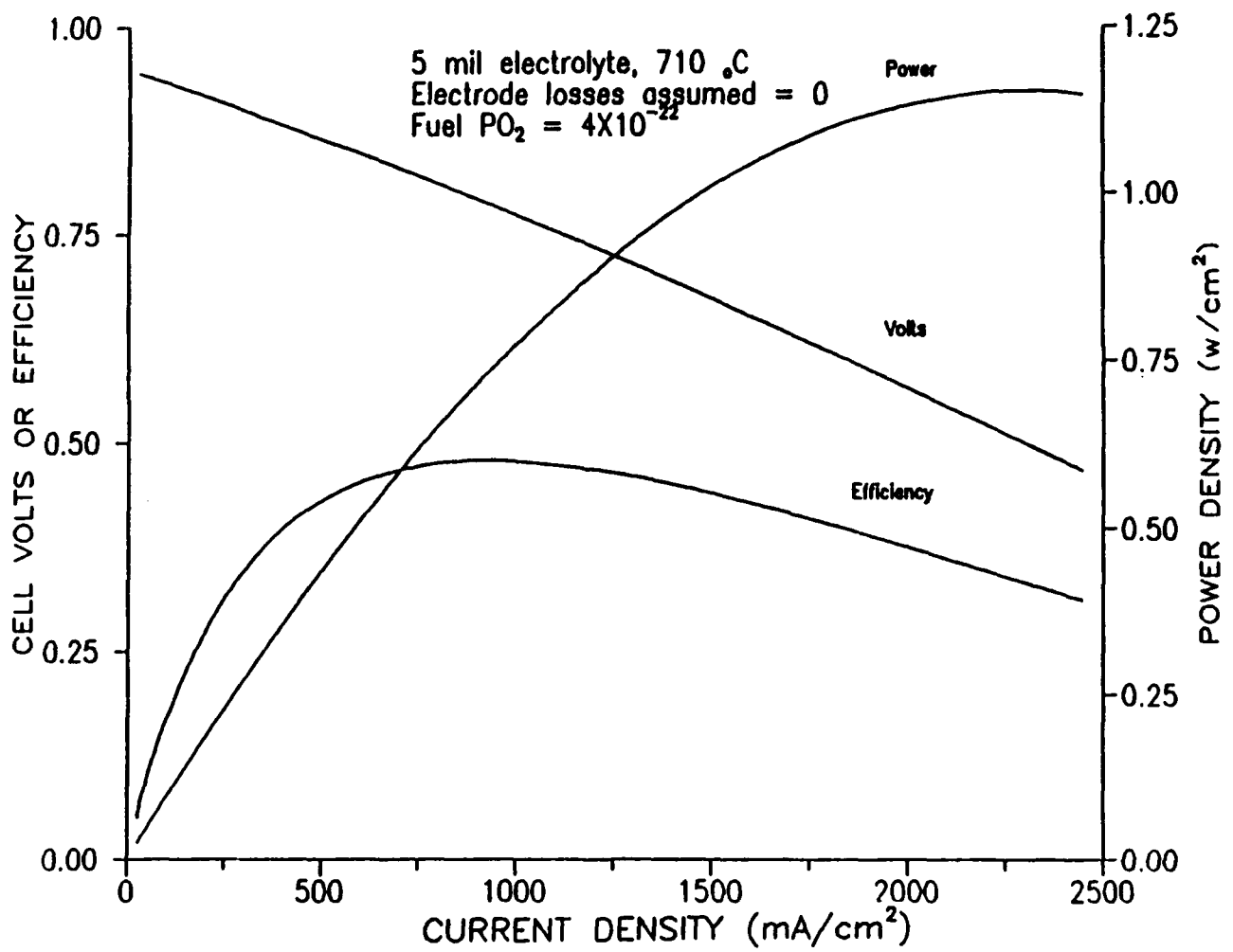


Figure 15. Estimated Ceria Electrolyte Performance

REFERENCES

- (1) "Conduction in Heterogeneous Systems," Meredith, R. E., and Tobias, C. W., in *Advances in Electrochemistry and Electrochemical Engineering*, Tobias and Delahay ed, Vol 2, Interscience Publishers, (1962) pp 15 - 45.
- (2) Tuller, H. L., and Nowick, J. *Electrochem. Soc.*, 122 No 2 pp 255-259, (1975).
- (3) Kudo, T., and Obayashi, J. *Electrochem. Soc.*, 123 No 3 pp 415-419, (1976)
- (4) Gerhardt et al. *J. Am. Ceram. Soc.* 69 pp 647-651, (1986)
- (5) Wang, D., Y., and Nowick A., S., *J. Solid State Chem.* 35 pp 325-333, (1980)
- (6) Selmi, F. A., and Amarakoon, V. R. W., *J. Am. Ceram. Soc.* 71 pp 943-937, (1988)
- (7) Selmi, F. A., and Amarakoon, V. R. W., *Ceramic Engineering and Science Proceedings* 8 September-October, (1987)
- (8) Ross, P. N. Jr., and Benjamin, T., G., *J. Power Sources*, 1 (1976-1977) pp 311-321

BIBLIOGRAPHY

IONIC CONDUCTIVITY

- Murray, A.D., Murch, G.E. and Catlow, C.R.A., "A New Hybrid Scheme of Computer Simulation Based on Hades and Monte Carlo: Application to Ionic Conductivity in Y^{3+} Doped CeO_2 ." Solid State Ionics, Vol. 18 and 19, pp. 196-202, 1986.
- Hilert, M. and Jansson, B., "Thermodynamic Model for Nonstoichiometric Ionic Phases - Application to CeO_{2-x} ." J. Am. Ceram. Soc., Vol. 69, pp. 732-34, 1986.
- Gerhardt-Anderson, R. and Nowick, A.S., "Ionic Conductivity of CeO_2 with Trivalent Dopants of Different Ionic Radii." Solid State Ionics, Vol. 5, pp. 547-550, 1981.
- Wang, D.Y., Park, D.S., Griffith, J. and Nowick, A.S., "Oxygen-Ion Conductivity and Defect Interactions in Yttria-Doped Ceria." Solid State Ionics, Vol. 2, pp. 95-105, 1981.
- Wang, D.Y. and Nowick, A.S., "Dielectric Relaxation from a Network of Charged Defects in Dilute $CeO_2:Y_2O_3$ Solid Solutions." Solid State Ionics, Vol. 5, pp. 551-554, 1981.
- Gerhardt, R., Lee, W.K. and Nowick, A.S., "Anelastic and Dielectric Relaxation of Scandia-Doped Ceria." J. Phys. Chem. Solids, Vol. 48, No. 6, pp. 563-569, 1987.

MIXED IONIC-ELECTRONIC CONDUCTIVITY

- Stratton, T.G. and Tuller, H.L., "Thermodynamic and Transport Studies Mixed Oxides, The CeO_2-UO_2 System." J. Chem. Soc., Faraday Trans. 2, Vol. 83, pp. 1143-1156, 1987.
- El-Houte, S. and El-Sayed Ali, M., "EMF Measurements on Gadolina Doped Ceria." Ceramics International, Vol. 13, pp. 243-246, 1987.
- Tuller, H.L., "Mixed Conduction in Nonstoichiometric Oxides," page 271, in Nonstoichiometric Oxides. edited by O. Toft Sorensen, Academic Press, 1981.
- Tuller, H.L. and Nowick, A.S., Ionic Conductivity of Doped Cerium Dioxide. Henry Krumb School of Mines, Columbia University, New York, New York.
- Tuller, H.L. and Nowick, A.S., "Doped Ceria as a Solid Oxide Electrolyte." Journal of the Electrochemical Society, Vol. 122, No. 2, pp. 255-259, February 1975.

- Ota, Y. and Butler, S.R., "Reexamination of Some Aspects of Thermal Oxidation of Silicon." Journal of the Electrochemical Society, Vol. 121, No. 8, pp. 1107-1111, June 1975.
- VanHandel, G.J. and Blumenthal, R.N., "The Temperature and Oxygen Pressure Dependence of the Ionic Transference Number of Nonstoichiometric $Ce_{1-x}O_{2-x}$." Journal of the Electrochemical Society, Vol. 121, No. 9, pp. 1198-1202, June 1975.
- Kudo, T. and Obayashi, H., "Oxygen Ion Conduction of the Fluorite-Type $Ce_{1-x}Ln_xO_{2-x/2}$ (Ln = Lanthanoid Element)." Journal of the Electrochemical Society, Vol. 122, No. 1, pp. 142-147, March 1976.
- Kudo, T. and Obayashi, H., "Mixed Electrical Conduction in the Fluorite-Type $Ce_{1-x}Gd_xO_{2-x/2}$." Journal of the Electrochemical Society, Vol. 123, No. 3, pp. 415-419, March 1976.
- Tuller, H.L. and Nowick, A.S., "Defect Structure and Electrical Properties of Nonstoichiometric CeO_2 Single Crystals." Journal of the Electrochemical Society, Vol. 126, No. 2, February 1979.
- Tuller, H.L. and Nowick, A.S., "Small Polaron Electron Transport in Reduced CeO_2 Single Crystals." J. Phys. Chem. Solids, Vol. 38, pp. 859-867, 1977.

CERIA RELATED MIXED CONDUCTION SYSTEMS

- Roth, R.S., Negas, T., Parker, H.S., Minor, D.B., Olson, C.D. and Skarda, C., "Phase Relationships and Crystal Chemistry of Compounds Containing Cerium Oxide," in The Rare Earths in Modern Science and Technology, edited by McCarthy, G.J. and Rhyne, J.J., Plenum, New York, 1978.
- Fujimoto, H.H. and Tuller, H.L., "Mixed Ionic and Electronic Transport in Thoria Electrolytes," in Fast Ion Transport in Solids, edited by Vashisha, Mundy, Shenoy of Elsevier North Holland, Inc., 1979.

CERIA FUEL CELLS

- Make, Y., Matsuba, M. and Kudo, T., Solid Electrolyte Fuel Cell, U.S. Patent No. 3,607,424, September 21, 1971.

Ross, Jr., P.N. and Benjamin, T.G., "Thermal Efficiency of Solid Electrolyte Fuel Cells with Mixed Conduction." Journal of Power Sources, Vol. 1, pp. 311-321, 1976/77.

Advanced Technology Fuel Cell Program, Final Report to the Electric Power Research Institute, Contract RP114, pp. 29-36, 1976.

Arai, H., Eguchi, K., Yahiro, H. and Baba, Y., High Temperature Fuel Cell with Ceria-Based Solid Electrolyte, presented at the Honolulu, Hawaii Meeting of the Electrochemical Society, October 18-23, 1987.

Yahiro, H., Baba, Y., Eguchi, K. and Arai, H., "High Temperature Fuel Cell with Ceria-Yttria Solid Electrolyte," Journal of the Electrochem. Soc., Vol. 135, No. 8, pp. 2077-2080, August, 1988.

CERIA GRAIN BOUNDARY EFFECTS

Duran, P., Jurado, J.R., Pascual, C., Rodrigues, J.M. and Moure, C., "Microstructural and Electrical Characterization of Some Ceria-Gadolinia Solid Electrolytes," in High Tech Ceramics, Elsevier Science Publishers B.V., Amsterdam, 1987.

Baumard, J.F., Gault, C. and Argoitia, A., "Sintered Ceria: A New Dense and Fine Grained Ceramic Material." Journal of the Less-Common Metals, Vol. 127, pp. 125-130, 1987.

Gerhardt, R. and Nowick, A.S., "Grain-Boundary Effect in Ceria Doped with Trivalent Cations: Electrical Measurements." Journal of the American Ceramic Society, Vol. 69, No. 9, pp. 641-46, September 1986.

Gerhardt, R. and Nowick, A.S., "Grain-Boundary Effect in Ceria Doped with Trivalent Cations: II, Microstructure and Microanalysis." Journal of the American Ceramic Society, Vol. 69, No. 9, pp. 647-51, September 1986.

Tanaka, J., Baumard, J.F. and Abelard, P., "Nonlinear Electrical Properties of Grain Boundaries in an Oxygen-Ion Conductor ($\text{CeO}_2 \cdot \text{Y}_2\text{O}_3$)" Journal of the American Ceramic Society, Vol. 70, No. 9, pp. 637-43, September 1987.

Wang, D.Y. and Nowick, A.S., A Grain-Boundary-Type Maxwell-Wagner Peak in the Thermally-Stimulated Depolarization of Doped Ceria Ceramics, Henry Krumb School of Mines, Columbia University, New York, New York, 1982.

- Wang, D.Y. and Nowick, A.S., "The 'Grain-Boundary' Effect in Doped Ceria Solid Electrolytes." Journal of Solid State Chemistry, Vol. 35, pp. 325-333, 1980.
- Butler, E.P. and Heuer, A.H., "Grain-Boundary Phase Transformations During Aging of a Partially Stabilized ZrO_2 - A Liquid-Phase Analogue of Diffusion-Induced Grain-Boundary Migration (DIGM) (?)." Journal of the American Ceramic Society, Vol. 68, No. 4, pp. 197-202, 1985.
- Verkerk, M.J., Middelhuis, B.J. and Burggraaf, A.J., "Effect of Grain Boundaries on the Conductivity of High Purity $ZrO_2 - Y_2O_3$ Ceramics." Solid State Ionics, Vol. 6, pp. 159-170, 1982.

CERIA ELECTRODE POLARIZATION PHENOMENA

- Wang, D.Y. and Nowick, A.S., Cathodic and Anodic Polarization Phenomena at Platinum Electrodes with Doped Ceria as the Electrolyte. Henry Krumb School of Mines, Columbia University, New York, New York.
- Wang, D.Y. and Nowick, A.S., Polarization Phenomena Associated with Reduction of a Doped Ceria Electrolyte. Henry Krumb School of Mines, Columbia University, New York, New York.
- Wang, D.Y. and Nowick, A.S., "Dielectric Relaxation in Yttria-Doped Ceria Solid Solutions." Journal Phys. Chem. Solids, Vol. 44, No. 7, pp. 639-646, 1983.
- Wang, D.Y. and Nowick, A.S., "Cathodic and Anodic Polarization Phenomena at Platinum Electrodes with Doped CeO_2 as Electrolyte." Journal Electrochem. Soc., Vol. 126, No. 7, pp. 1155-1165, July 1979.
- Wang, D.Y. and Nowick, A.S., "Cathodic and Anodic Polarization Phenomena at Platinum Electrodes with Doped CeO_2 as Electrolyte II. Transient Overpotential and A-C Impedance." Journal Electrochem. Soc., Vol. 126, No. 7, pp. 1166-1172, July 1979.
- Wang, D.Y. and Nowick, A.S., "Diffusion-Controlled Polarization of Pt, Ag, and Au Electrodes with Doped Ceria Electrolyte." Journal Electrochem. Soc., Vol. 128, No. 1, pp. 55-63, January 1981.

Knappe, P. and Eyring, L., "Preparation and Electron Microscopy of Intermediate Phases in the Interval $Ce_{7}O_{12}$ - $Ce_{11}O_{20}$." Journal of Solid State Chemistry, Vol. 58, pp. 312-324, 1985.

CERIA PHASE DIAGRAMS AND THERMODYNAMIC PROPERTIES

Daniel, D.W., "Infrared Studies of CO and CO_2 Adsorption on Pt/ CeO_2 : The Characterization of Active Sites." Journal Phys. Chem., Vol. 92, No. 13, pp. 3891-3899, 1988.

Negas, T., Roth, R.S., McDaniel, C.L. Parker, H.S. and Olsen, C.D., Oxidation-Reduction Reactions of $CeMO_{4+x}$ (M = Ta or Nb Phases, National Bureau of Standards Mat. Res. Bull., Vol. 12, pp. 1161-1171, 1977.

Cava, R.J., Negas, T., Roth, R.S. and Parker, H.S., "Crystal Chemistry and Oxidation-Reduction in Phases in Rare Earth Tantalate-Niobate Systems," in The Rare Earths in Modern Science and Technology, edited by McCarthy, G.J. and Rhyne, J.J., Plenum, New York, 1978.

Mizuno, M., Yamada, T. and Noguchi, T. "Phase Diagram of the System Al_2O_3 - Pr_2O_3 at High Temperature." Nagoya Kogyo Gijutsu Shikensho Hokoku, Vol. 27, No. 2, pp. 47-52, 1978.

Chaminade, J.P., Olazcuaga, R., LePolles, G., LeFlem, G. and Hagenmuller, P., "Crystal Growth and Characterization of $Ce_{1-x}Pr_xO_2$ (x 0.05) Single Crystals." Journal of Crystal Growth, Vol. 87, pp. 463-465, 1988.

McCullough, J.D. and Britton, J.D., "X-Ray Studies of Rare Earth Oxide Systems. II. The Oxide Systems $Ce^{IV}-Sm^{III}$, $Ce^{IV}-Gd^{III}$, $Ce^{IV}-Y^{III}$, $Pr^{IV}-Y^{III}$ and $Pr^{III}-Y^{III}$." American Chem. Soc. Journal, Vol. 74, pp. 5225-5227, 1952.

Lopato, L.M., Lugin, L.I. and Shevchanko, A.V., "Phase Diagram of the Praseodymium Sesquioxide-Calcium Oxide System." Russian Journal of Inorganic Chemistry, Vol. 17, No. 9, pp. 2543-2545, 1972.

DISTRIBUTION LIST

Director
Advanced Research Project Agency
1400 Wilson Boulevard
Arlington, Virginia 22209
Attn. Dr. David Squire
(2 Copies)

Administrative Contracting Officer
DCASMA-Hartford
96 Murphy Road
Hartford, CT 06114-2173
(1 copy)

Defense Technical Information Center
Bldg. 5, Cameron Station
Alexandria, Virginia 22314
(2 Copies)

Director
Naval Research Laboratory
Attn. Code 2627
Washington, D. C. 20375
(1 Copy)

APPENDICES

APPENDIX A

New York State College of Ceramics
at Alfred University
Alfred, N.Y. 14802

Report on Zirconia Gel Coating of Cerium Oxide Powders

V.R.W. Amarakoon

J. Neely III

11/20/89

Objective

Cerium powders used in solid electrolyte fuel cells tend to allow electronic conductivity under reducing PO_2 conditions and this is detrimental to the cell's performance. Sol-gel coating of the cerium oxide with zirconia was attempted in hopes of resisting the valance change in the cerium oxide which leads to the backflow in the cell. The objective was to provide a protective skin (i.e. barrier) of zirconia around the ceria particles which would provide for a valance stability while not decreasing ionic conductivity.

Procedure

Experiments were performed to optimize the zirconia sol-gel system to be used in the coating process. Emphasis was placed on the development of a clear gel which formed in less than two hours with proven reproducibility. The system selected for the coating process consisted of zirconium n-butoxide butanol diluted in propanol in the ratio 1:3. The pH of the solution was lowered to a range between 2-3 by the addition of concentrated nitric acid. Upon the addition of 1ml of water per 20 ml of zirconium n-butoxide butanol, the system gelled in the required time with no visible precipitation of zirconia.

For the purpose of coating the ceria powders, three mole percent of yttrium nitrate was also included in the gel-preparation. The total gel used in coating the ceria powders equaled three mole percent of the ceria to be coated.

Coating was achieved by first mixing the gel-solution for ten minutes after the yttrium addition dissolved. The solution was then added to the ceria powders with excess alcohol and ball milled with zirconia media for two hours. After separating the slurry from the media, water was added in the proportion previously stated, and the solution was magnetically stirred until the gellation occurred.

The gelled mass was air dried, crushed, and dried at 60 C for several days before final grinding and sieving through a 325 mesh screen. These powders were then turned over to National Fuel Cell where they were pressed into disks and sintered.

Two sample disks were returned to Alfred University for characterization. STEM analysis was carried out on thin sections of the coated and uncoated samples provided. Figures 1 and 2 show TEM micrographs of coated and uncoated samples, respectively, which exhibit well sintered grains and the absence of second phases in the grain boundary regions. Electron dispersive spectrometry (EDS) revealed a uniform distribution of zirconia in the grain boundaries, triple point regions, and on the grain surfaces of the coated disk. No zirconium was detected in the uncoated disk, as would be expected. Figures 3-6 provide the EDS analysis results for a grain boundary, grain surface and triple point region in the coated sample, and a triple point region of the uncoated sample, respectively.

Given these results, it seems likely that a skin which existed prior to sintering formed a solid solution with the ceria during the sintering process. This assumption is further strengthened by examination of the cerium oxide-zirconium oxide phase diagram which

shows wide ranges of solid solution formation (see Figure 7). The formation of this solid solution defeats the effort to provide a protective skin; therefore, it appears unlikely that this method of gel coating is applicable to National Fuel Cell's needs unless the solid solution formation can be prevented. A possible solution to this problem may come from:

- a. Adjustment of coating layer composition
- b. Adjustment of sintering profile

Specific attention must be paid to the adjustment of the sol-gel composition, in which a liquid phase may be incorporated which could crystallize into a ZrO_2 based composition on annealing. However, the sintering profile needs to be adjusted so that liquid phase sintering could take place with subsequent fast cooling to allow for the liquid phase so developed to remain in the grain boundary region. These regions could be annealed in a subsequent firing to crystallize the ZrO_2 phase.



Figure 1-TEM Photograph of Sintered, Coated Powder



Figure 2-TEM Photograph of Sintered, Uncoated Powder

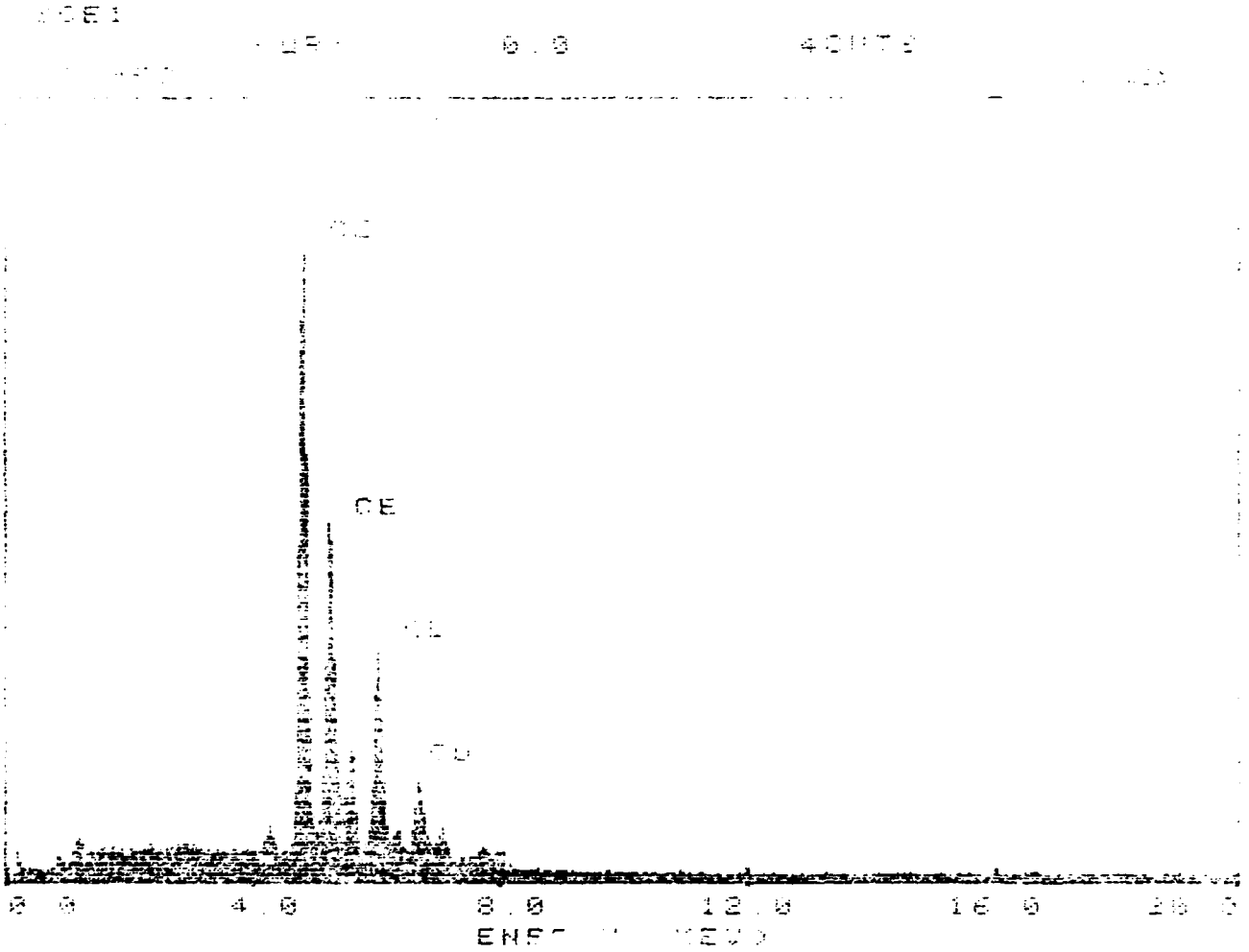


Figure 3-EDS of Grain Boundary Region: Coated Powder

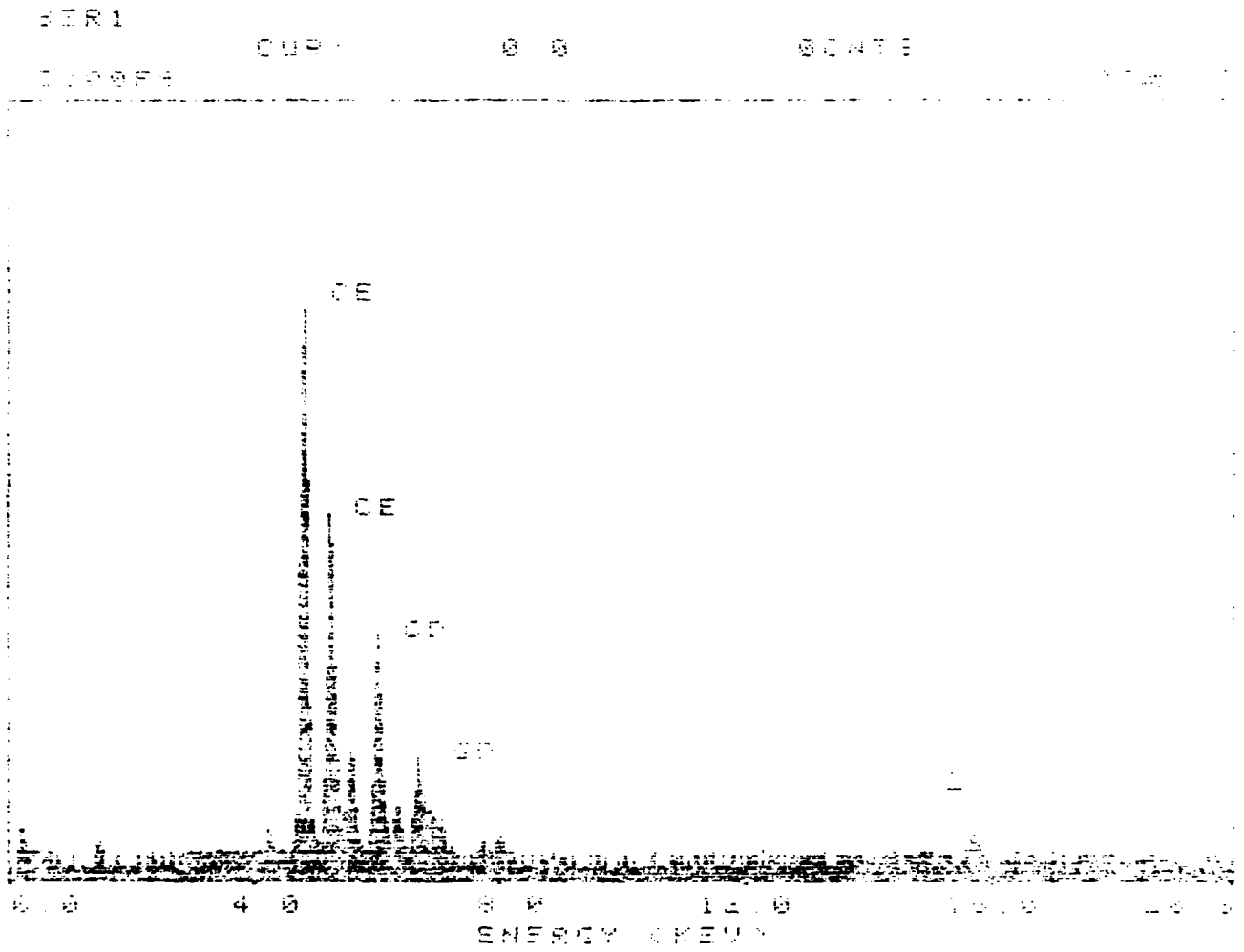


Figure 4-EDS of Grain: Coated Powder

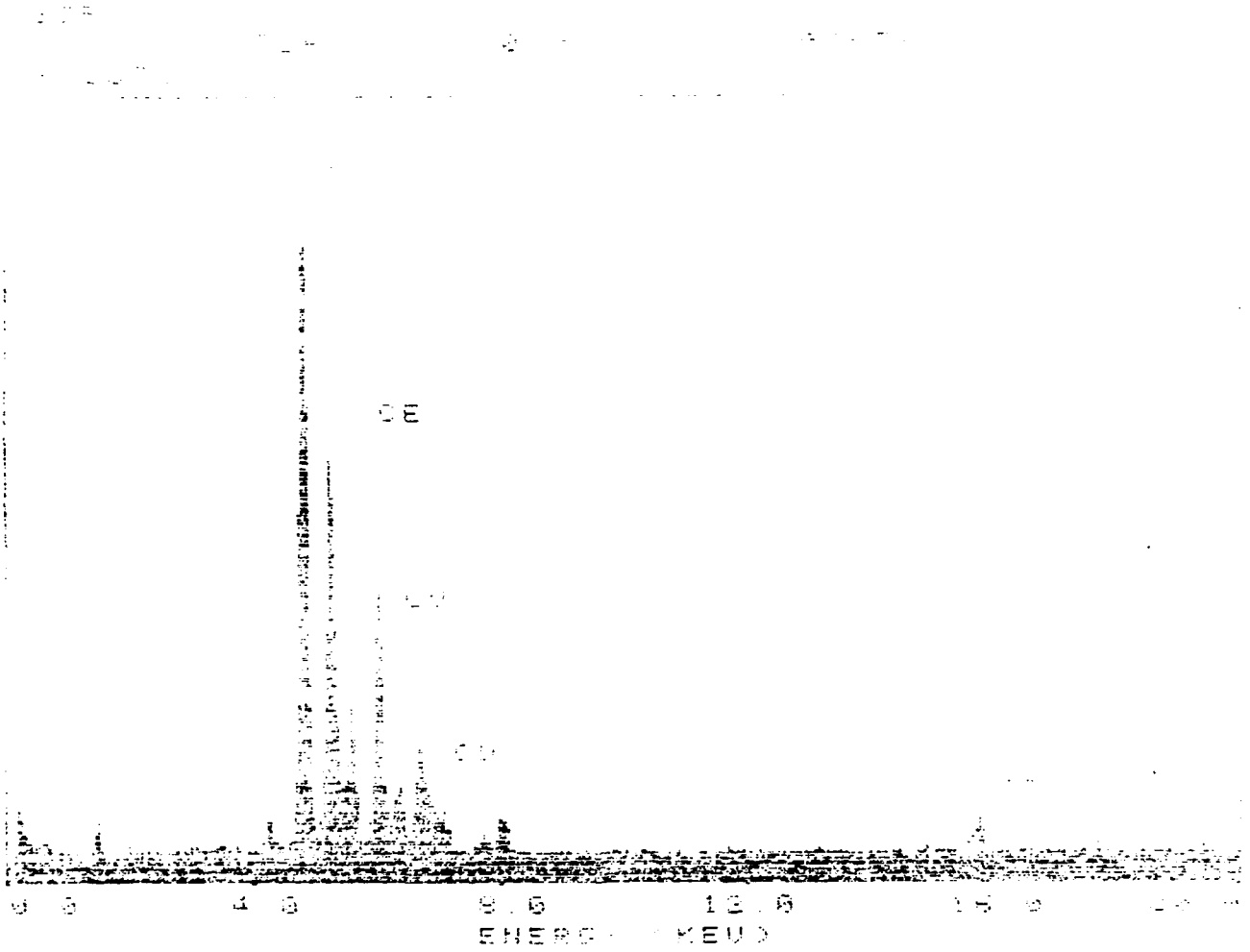


Figure 5-EDS of Triple Point Region: Coated Powder

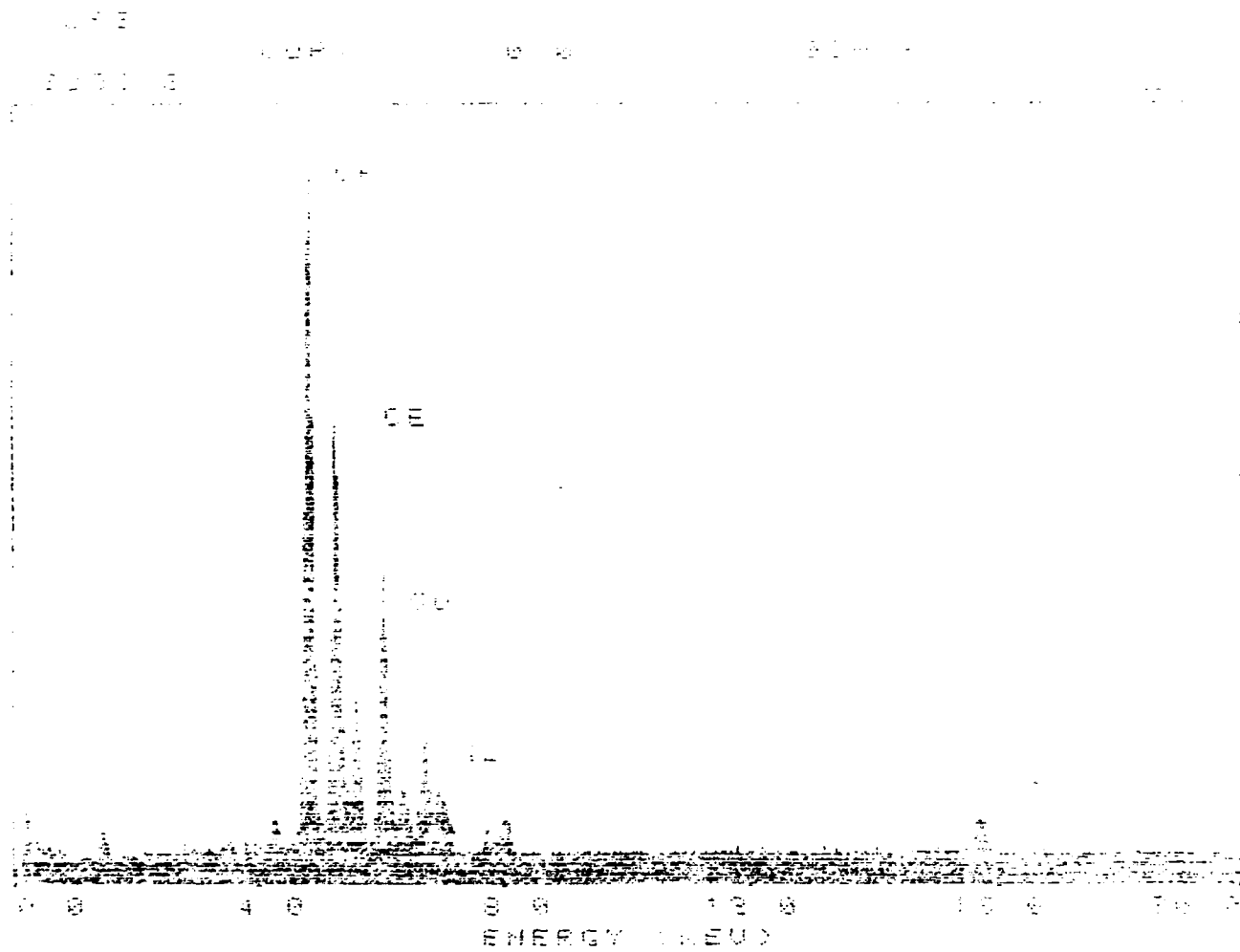


Figure 6-EDS of Triple Point Region: Uncoated Powder

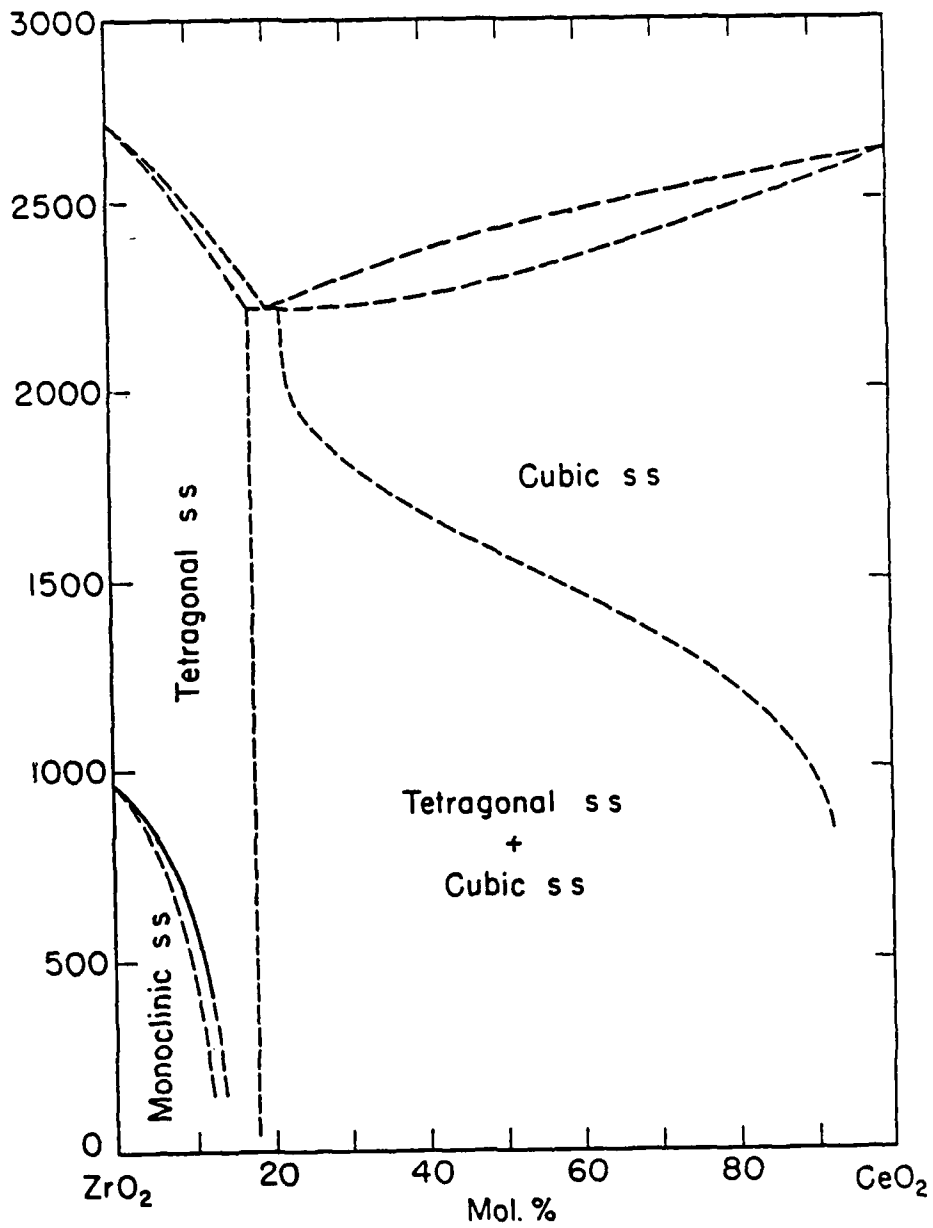


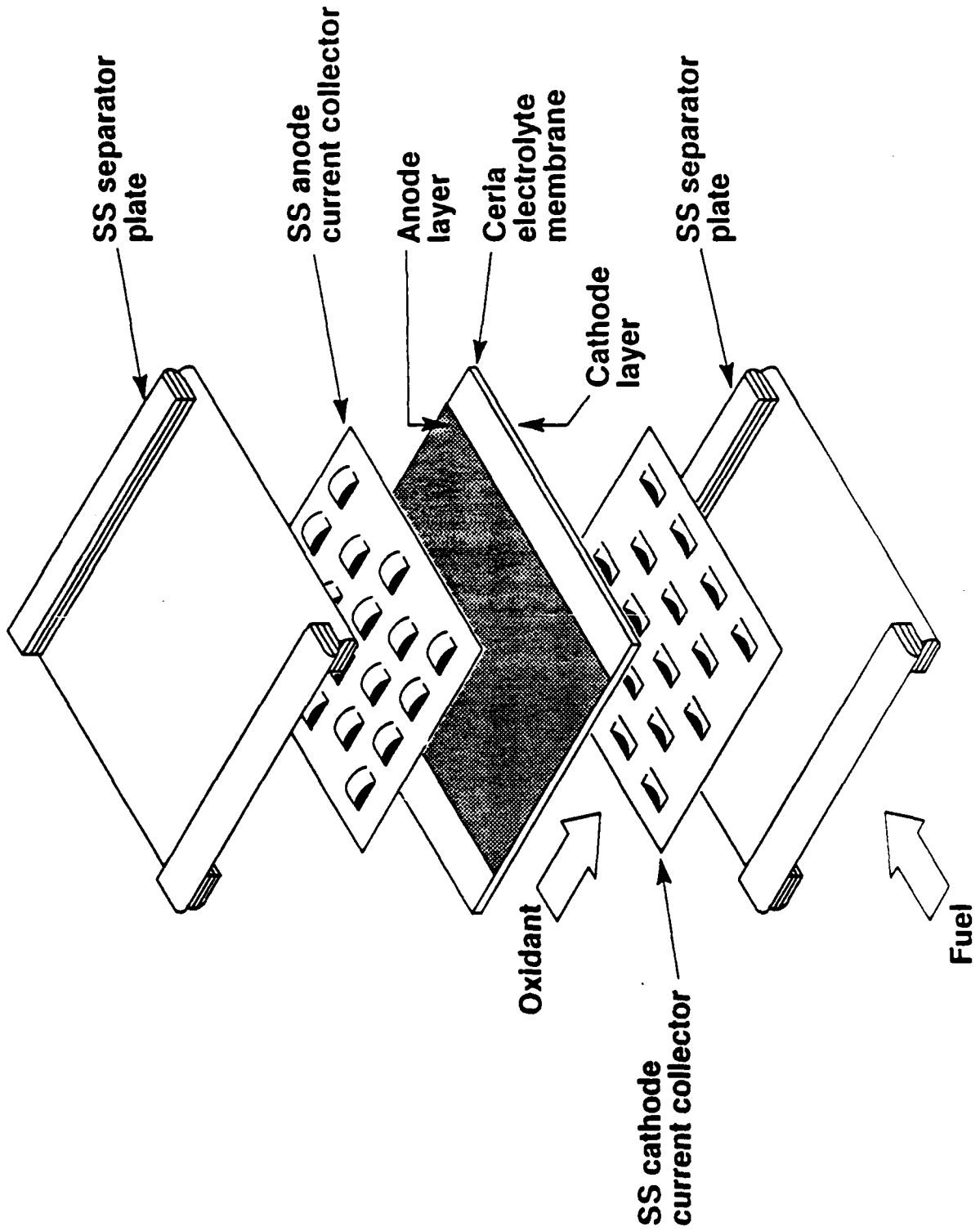
FIG. 127.—System CeO₂-ZrO₂.

Pol'Duwez and Francis Odell, *J. Am. Ceram. Soc.*, 33 [9] 280 (1950).

Figure 7-Phase Diagram for Cerium and Zirconium Oxides

APPENDIX B

CERIA CELL CONCEPT



CERIA ELECTROLYTE DEVELOPMENT PLAN

- 0 PHASE I - 18 MONTHS, ENDED DECEMBER 1989
DEVELOPED ELECTROLYTE COMPOSITION WHICH LOWERED
ELECTRONIC SHORT TO ACCEPTABLE LEVELS

- 0 FISCAL 1990 PROGRAM
DEVELOP THIN ELECTROLYTE DISC
DEVELOP CATHODE
TEST DISC CELL

- 0 FISCAL 1991 PROGRAM 12 MO
OPTIMIZE ANODE
SCALE UP & FAB PARTS FOR 1KW-SCALE SINGLE CELL TEST
DESIGN SHEET METAL PARTS
DEVELOP SEALS
TEST 1 KW-SCALE SINGLE CELL

0 FISCAL '92 - '93 1 KW-STACK PROGRAM
STACK DESIGN
REPEAT PART PROCESS DEVELOPMENT
FABRICATION
TEST

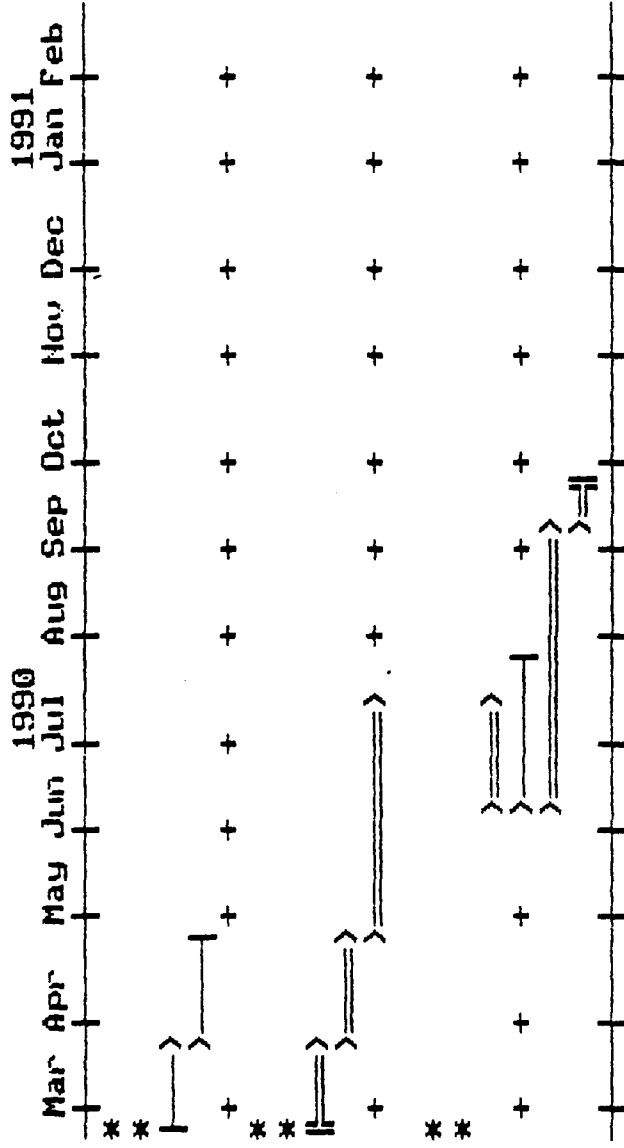
1990 CERIA PROGRAM PLAN

- O TASK I ELECTROLYTE DEVELOPMENT AND FABRICATION
DEVELOP FABRICATION PROCESSES
FABRICATE ELECTROLYTES FOR TASKS II AND III

- O TASK II DEVELOP A CATHODE FOR THE CERIA CELL
PROCURE CANDIDATE MATERIALS
 - NIOBIUM DOPED CERIA
 - STRONTIUM DOPED LANTHANUM MANGANATEDEVELOP SLURRY CAST APPLICATION TECHNIQUE
FABRICATE CATHODES FOR TESTING

- O TASK III CELL TEST CATHODES
DEVELOP CERIA DISC CELL SEAL
APPLY NI/ZIRCONIA ANODE
TEST DISC CELL
FINAL REPORT DOCUMENTING ELECTROLYTE FABRICATION
AND CATHODE DEVELOPMENT

OMR/DARPA CERIA PROGRAM
1990 PROGRAM PLAN



1
2
3
4
5
6
7
8
9
10
11
12
13
14
15
16
17

1991 CERIA PROGRAM PLAN

- O TASK I OPTIMIZE ANODE FOR CERIA CELL
SELECT CANDIDATE MATERIALS
 - UNDOPED CERIA
 - NICKEL ZIRCONIA CERMETDEVELOP FABRICATION TECHNIQUE
TEST DISC CELL

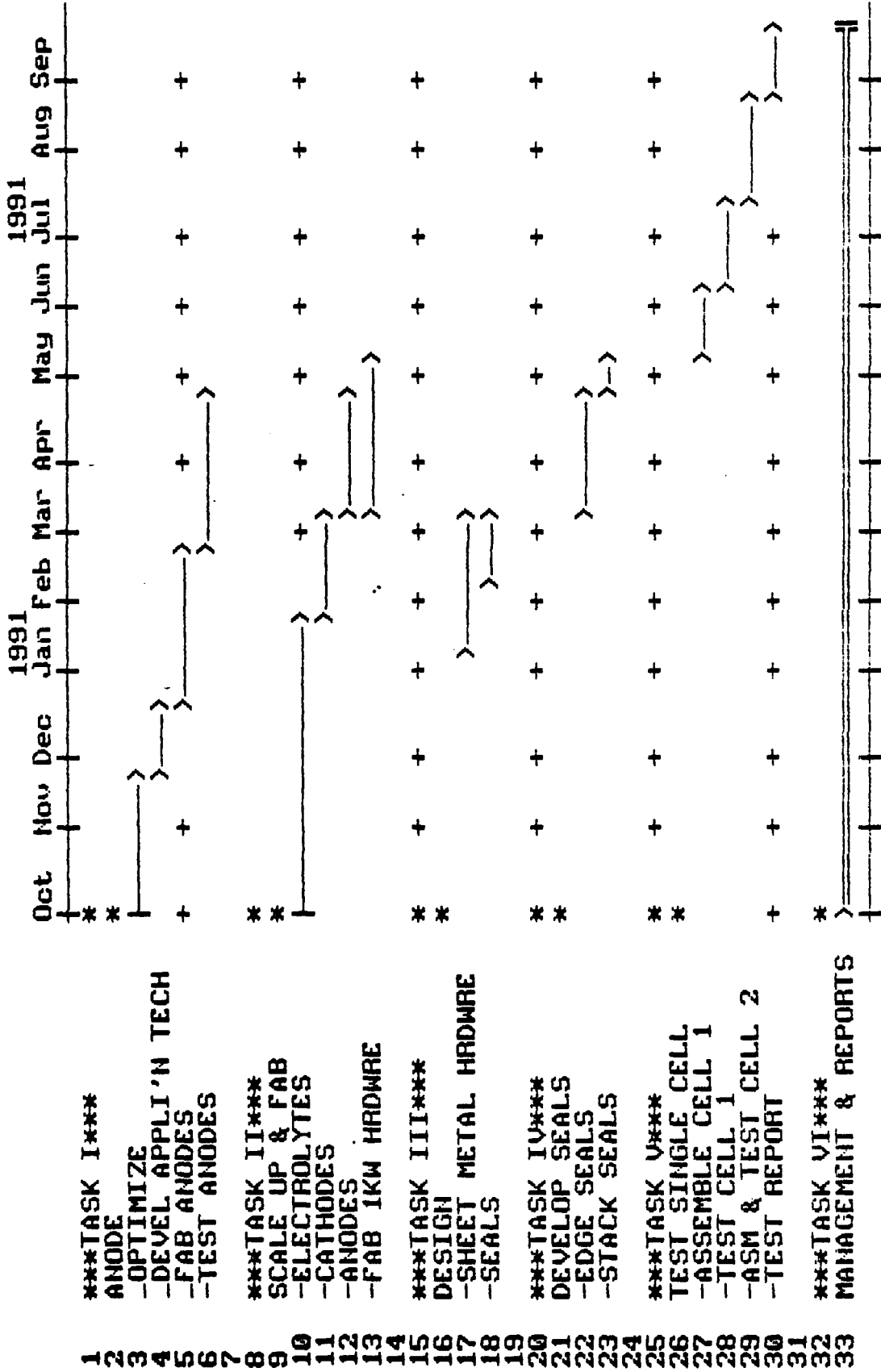
- O TASK II SCALE UP & FAB PARTS FOR 1KW SIZE CELL
ELECTROLYTES (NOMINAL 5x5 INCHES)
ANODES
CATHODES
SHEET METAL HARDWARE

- O TASK III DESIGN SHEET METAL SINGLE CELL COMPONENTS
CANDIDATE MATERIALS AND CONFIGURATIONS DERIVED FROM MOLTE
CARBONATE TECHNOLOGY

- 0 TASK IV DEVELOP SEALS
 - CELL EDGE SEALS
 - STACK GAS MANIFOLD SEALS
 - CANDIDATE SEALS FROM MOLTEN CARBONATE TECHNOLOGY

- 0 TASK V RUN 1KW SIZE SINGLE CELL TESTS
 - ASSEMBLE TEST CELLS
 - TEST

ONR/DARPA CERIA PROGRAM
1991 PROGRAM PLAN



1
2
3
4
5
6
7
8
9
10
11
12
13
14
15
16
17
18
19
20
21
22
23
24
25
26
27
28
29
30
31
32
33

1 KW-STACK CERIA PROGRAM PLAN

- 0 TASK I DESIGN STACK
 - CELL PACKAGE (ANODE/ELECTROLYTE/CATHODE)
 - SHEET METAL CURRENT COLLECTORS
 - SEPARATOR PLATES
 - SEALS

- 0 TASK II REPEAT PART PROCESS DEVELOPMENT
 - CELL PACKAGE
 - SHEET METAL

- 0 TASK III FABRICATION - 50 CELLS
 - CELL PACKAGE
 - CURRENT COLLECTORS
 - PLATES
 - SEALS
 - NON-REPEAT STACK HARDWARE

0 TASK IV 1-KW CERIA STACK TEST
MODIFY TEST STAND
STACK ASSEMBLY
STACK TEST

0 TASK V MANAGEMENT AND REPORTING

1 KN CERIA STACK PROGRAM PLAN
1992 - 1993

